



# Segmentation and localization of glioma growth in longitudinal mpMRI recordings

- with a view to generative AI in coding and interpretation

Prof. Arvid Lundervold BSc, MD, PhD

Department of Biomedicine  
Mohn Medical Imaging and Visualization Center  
University of Bergen  
Norway

*"At its most fundamental level, I think biology [and likely medicine] can be thought of as an information processing system, albeit an extraordinarily complex and dynamic one.*

*Just as mathematics turned out to be the right description language for physics, biology may turn out to be the perfect type of regime for the application of AI."*

- Sir Demis Hassabis, 2021



[Isomorphic Labs](#) / [Google DeepMind](#)



Nobel Prize in Chemistry, 2024

Precision medicine

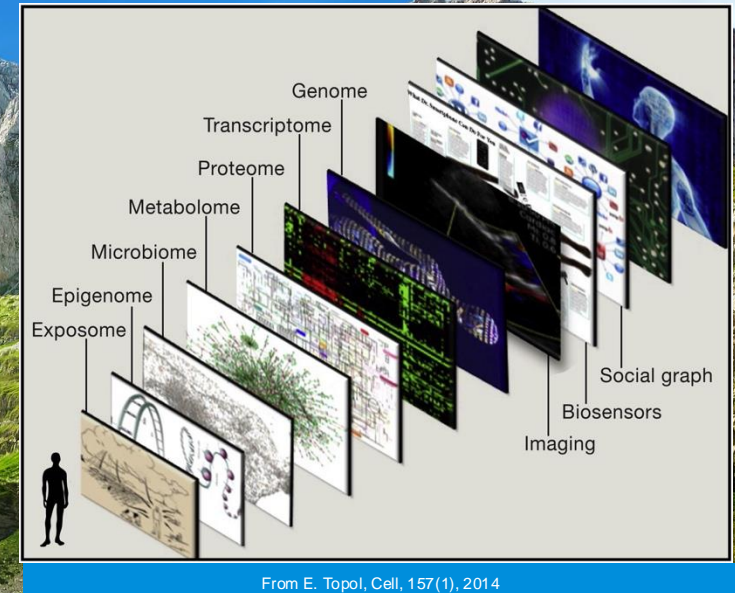
# bio-medical AI

Personalized medicine

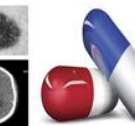
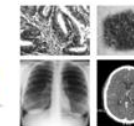
«Deep phenotyping»

«Deep medicine»

Future medicine



From cradle-to-grave  
from «lust to dust»



Stem cell  
and  
regene-  
rative  
medicine

Digital  
health  
data and  
registries

Wearable  
health/  
assistive  
living  
technology

Mental  
health  
and well-  
being

Pre-  
hospital  
services/  
home  
nursing

Radiology,  
Laboratory  
Digital  
Pathology

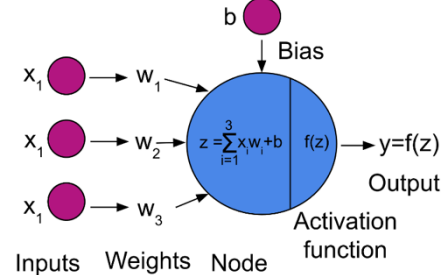
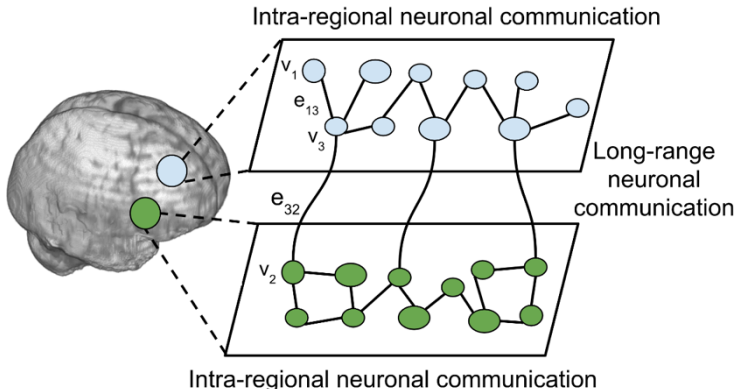
Novel  
drug  
discovery

Disease and  
patient  
stratification

Patient  
safety  
and risk

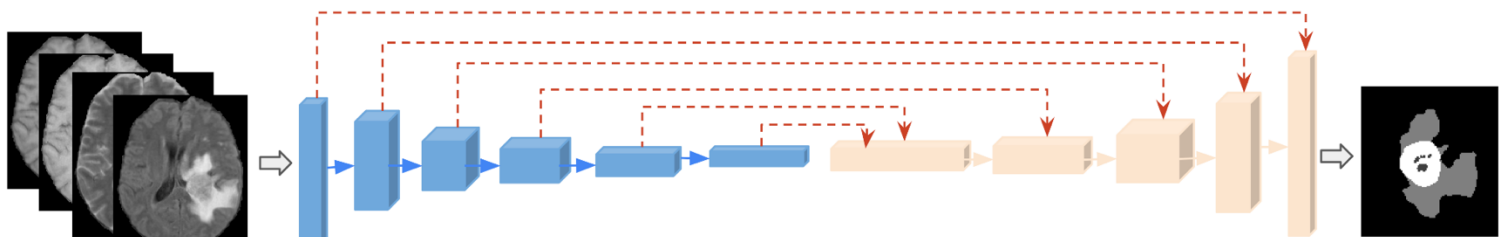
Hospital  
manage-  
ment

# Neural Networks in brain



# in machine

Multimodal  
MRI Input



(T1, T1c, T2, FLAIR)

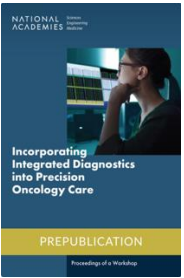
Encoder

Decoder

- (T1, T1c, FLAIR) — Encoder 2
- (T1, T1c, T2) — Encoder 3
- (T1, T2, FLAIR) — Encoder 4
- (T1c, T2, FLAIR) — Encoder 5

Adopted **multi-encoder** based **U-Net** architecture

# Integrated diagnostics ...



The convergence of imaging, pathology, and laboratory testing data, augmented with information technology, is referred to as **integrated diagnostics**

National Academies of Sciences, Engineering, and Medicine. 2024.  
*Incorporating Integrated Diagnostics into Precision Oncology Care: Proceedings of a Workshop.*  
Washington, DC:  
The National Academies Press.  
<https://doi.org/10.17226/27744>

Continuous Measurements and Modeling

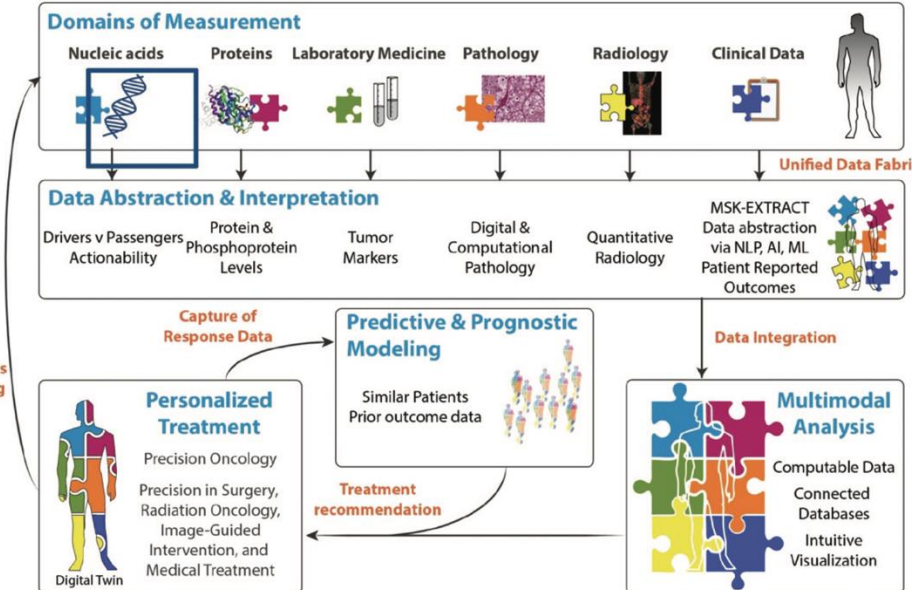


FIGURE 1 Integrated data science approach to personalized treatment.

<https://nap.nationalacademies.org/catalog/27744>

A possible methodological approach:

Graph Convolutional Networks in Multi-modality Medical Imaging: Concepts, Architectures, and Clinical Applications

Kexin Ding<sup>a</sup>, Mu Zhou<sup>b</sup>, Zichen Wang<sup>c,d</sup>, Qiao Liu<sup>e</sup>, Corey W. Arnold<sup>c,d</sup>, Shaotong Zhang<sup>f,\*</sup>, Dimitri N. Metaxas<sup>e,\*</sup>

<sup>a</sup>Department of Computer Science, UNC Charlotte, Charlotte, NC, USA

<sup>b</sup>Sensebrain Research, San Jose, USA

<sup>c</sup>Computational Diagnostics Lab, UCLA, Los Angeles, USA

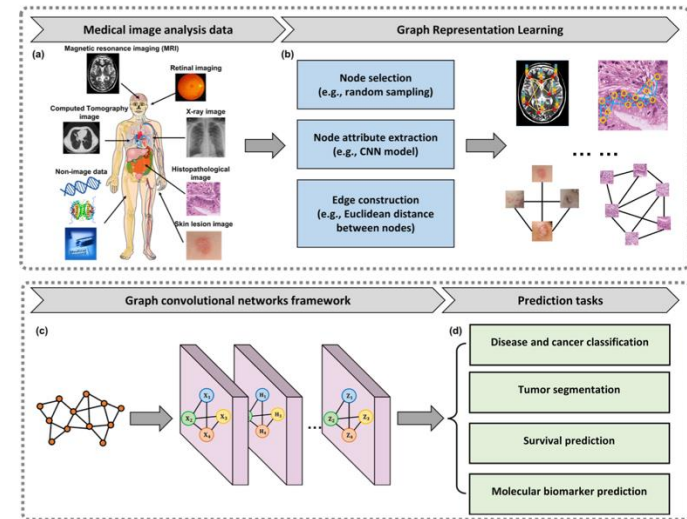
<sup>d</sup>Department of Bioengineering, UCLA, Los Angeles, USA

<sup>e</sup>Department of Statistics, Stanford University, Stanford, USA

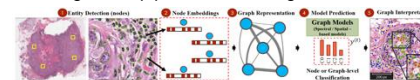
<sup>f</sup>Shanghai Artificial Intelligence Laboratory, Shanghai, China

<sup>\*</sup>Department of Computer Science, Rutgers University, New Jersey, USA

<https://arxiv.org/abs/2202.08916>



A general pipeline for utilizing GCNs in medical image analysis.



A Survey on Graph-Based Deep Learning for Computational Histopathology. (2022)

<https://www.sciencedirect.com/science/article/pii/S0895611211001762>

# Transformative role of AI in bio-medical laboratories

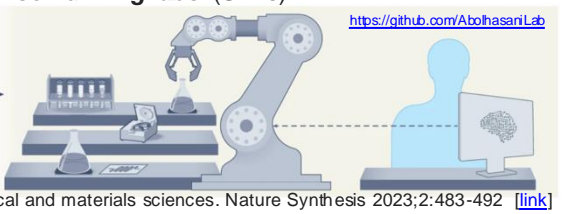
Wet lab - Dry lab - "Moist" lab - SDL

nature synthesis



M Abolhasani & E Kumacheva. The rise of self-driving labs in chemical and materials sciences. *Nature Synthesis* 2023;2:483-492 [link]

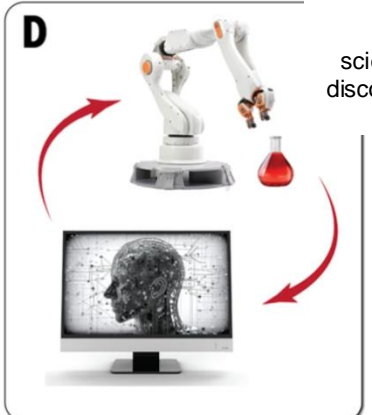
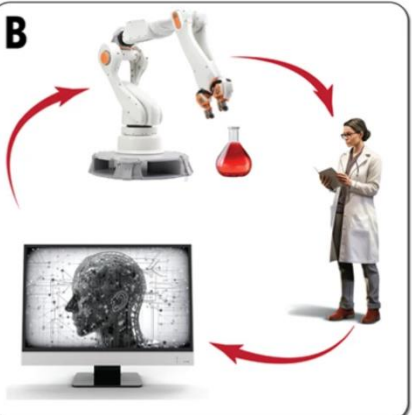
self-driving labs (SDLs)



<https://github.com/AbolhasaniLab>

nature communications

Degree of autonomy in “self-driving” laboratories (SDLs)



Can AI do scientific discoveries ?

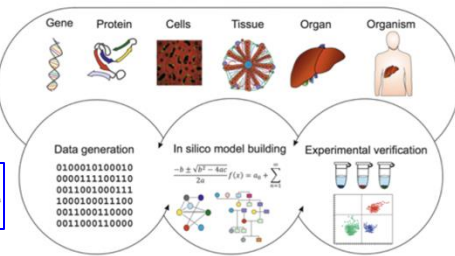
Jablonka et al.  
*Nat Mach Intell*  
2024

Wang et al.,  
*Nature* 2023



Illustration of workflow for each level (A) **piecemeal**, where human users completely separate the experiment and the computer system, (B) **semi-closed loop**, where the algorithm and the robot components partially communicate, (C) **closed loop**, where the human user has no influence in the targeting the loop, and (D)**self-motivated experimental systems**, where the computer system dictates its own goals.

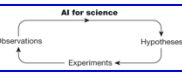
A A Volk & M Abolhasani. Performance metrics to unleash the power of self-driving labs in chemistry and materials science. *Nature Comm.* 2024;15:1378 [link] Arvid Lundervold



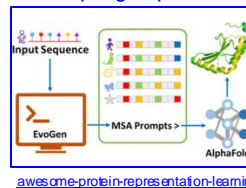
Data generation  
01000101000010  
00001111000110  
00110010001111  
1000100011100  
0011000110000  
0011000111000

In silico model building  
$$-\frac{b \pm \sqrt{b^2 - 4ac}}{2a} f(x) = a_0 + \sum_{k=1}^{n-1} a_k x^k$$

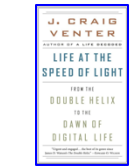
Experimental verification



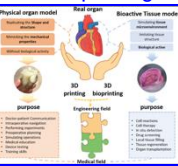
Prompting of proteins



*J. CRAIG VENTER*  
LIFE AT THE SPEED OF LIGHT



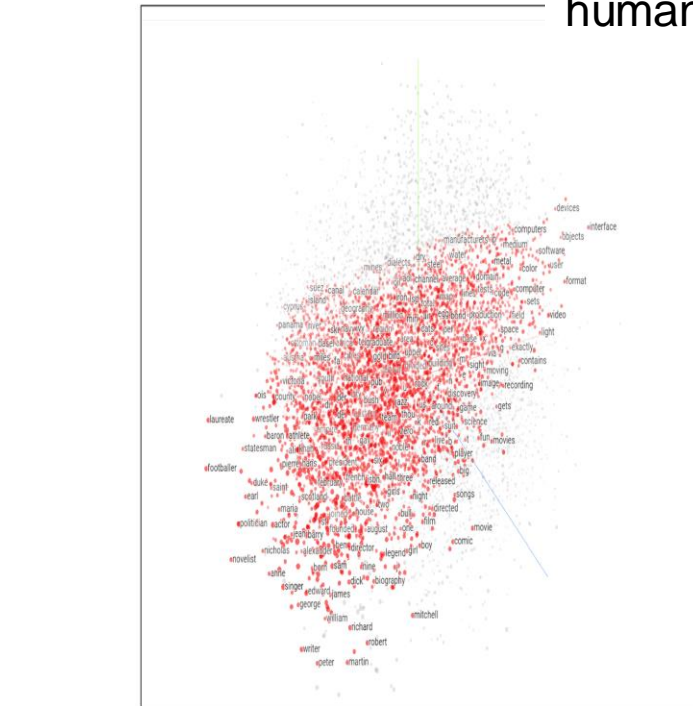
3D-bioprinting



# Deep learning and representations in human and machine

**Language**

See also UiB's [HBF Hjemme og Bevissthet Forum](#):  
"Representation learning and consciousness" [ [link](#) ]



'Dog'

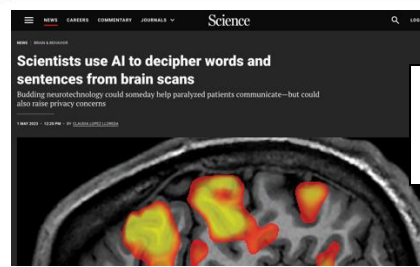
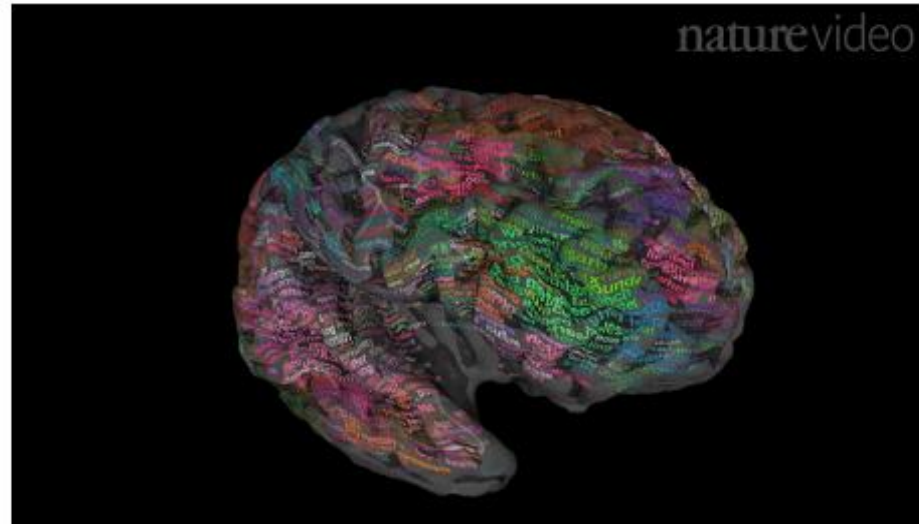


Word2Vec

5.12695312e-02	-2.23388672e-02	-1.72851562e-01	1.61132812e-01
-8.44726562e-02	5.73730469e-02	5.85937500e-02	-8.25195312e-02
-1.53808594e-02	-6.34765625e-02	1.79687500e-01	-4.23928125e-01
-2.25837678e-02	-1.66015625e-01	-2.51406844e-02	1.42421875e-01
-1.99187701e-02	-1.59319375e-01	-1.50090909e-02	-1.20717500e-01
1.55273438e-01	-9.91210531e-02	1.42578125e-01	1.64062500e-01
-8.93554688e-02	2.60105312e-01	1.49414062e-01	3.20312500e-01
3.28125000e-01	2.44140625e-02	-9.71679688e-02	-8.20312500e-02

(words and concepts maps to high-dimensional vectors of numbers)

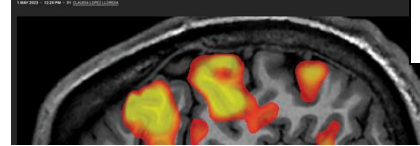
→ Jamali et al. Semantic encoding during language comprehension at single-cell resolution. [Nature 2024;631:610–616](#)



May 1<sup>st</sup> 2023 [The New York Times](#)

## A.I. Is Getting Better at Mind-Reading

In a recent experiment, researchers used large language models to translate brain activity into words.



<https://github.com/HuthLab/semantic-decoding>

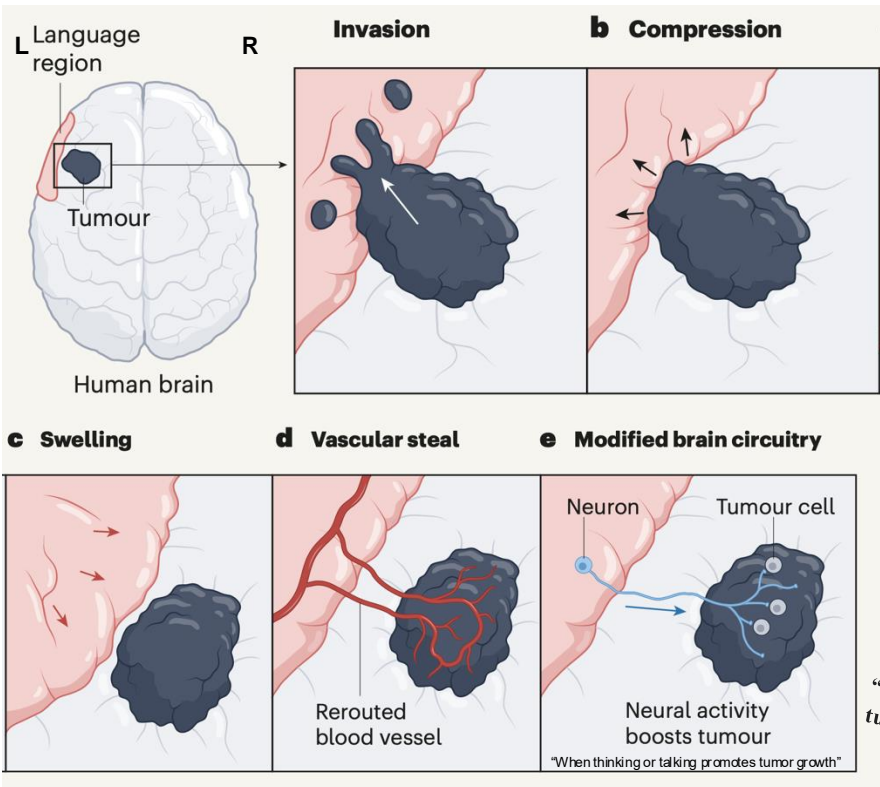
Tang et al. Semantic reconstruction of continuous language from non-invasive brain recordings.

[Nature Neuroscience 2023;26:858-866](#)

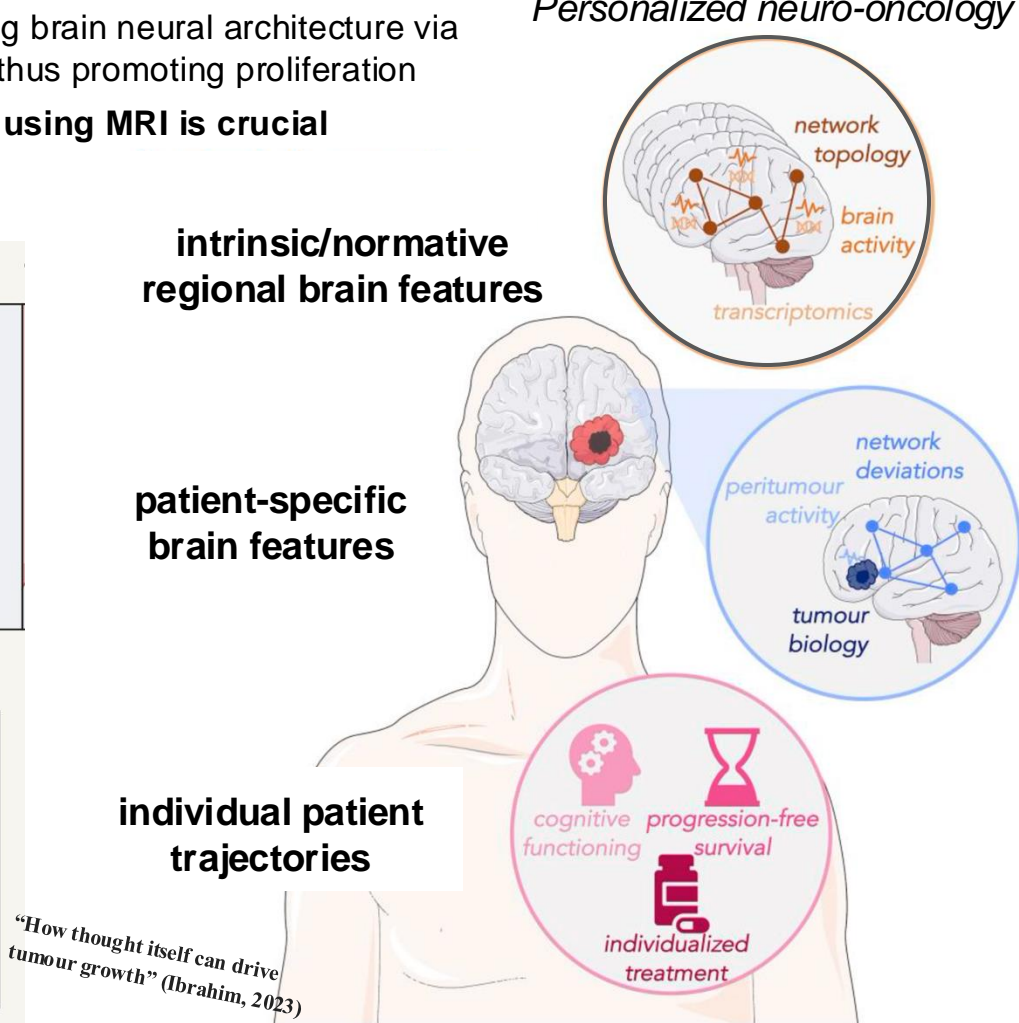
**Glioma potentially exploits neuroplasticity**, reshaping brain neural architecture via synaptic remodeling and increased neuronal signaling, thus promoting proliferation

**Accurate localization of glioma sub-compartments using MRI is crucial**

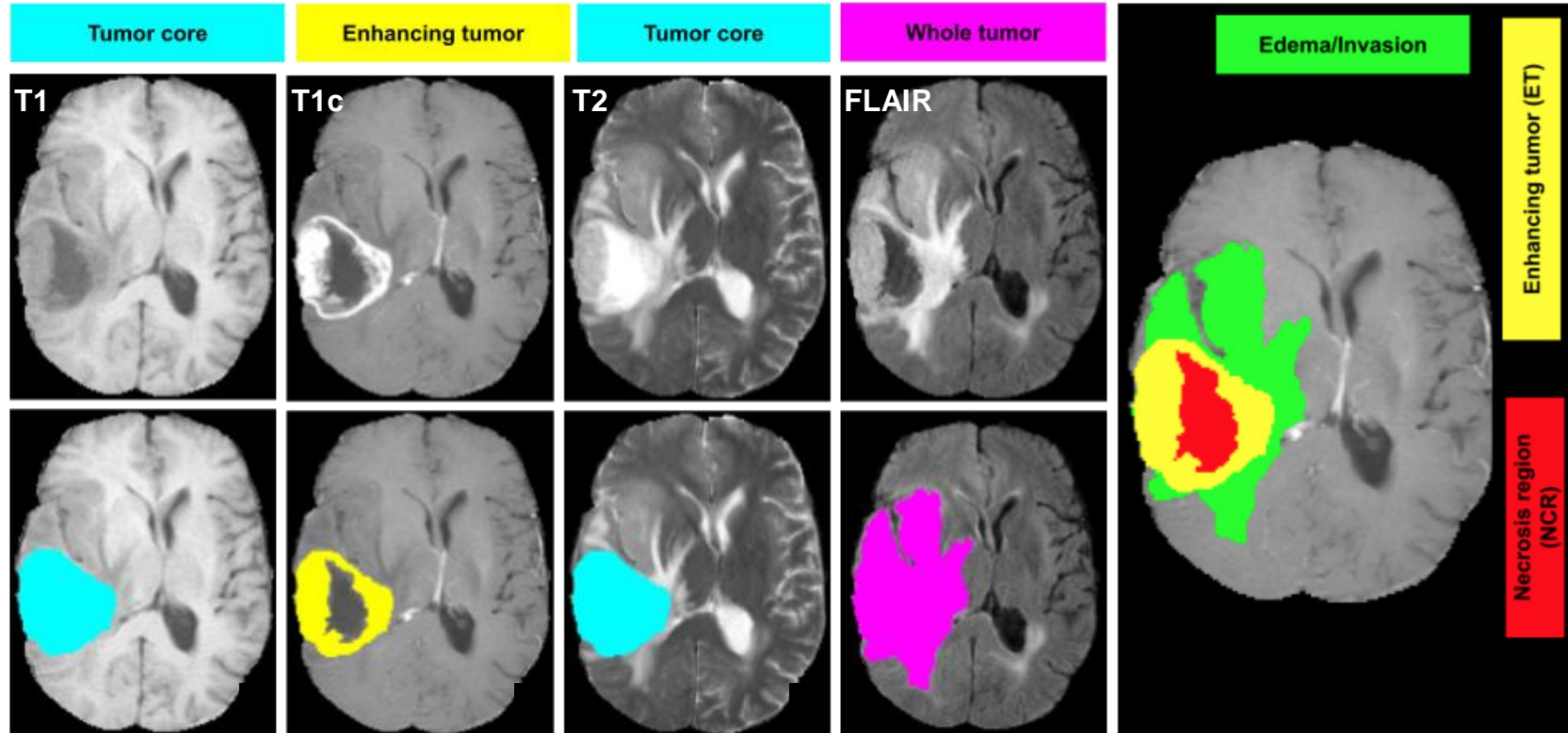
Mechanisms potentially affecting cognition due to tumor growth



Personalized neuro-oncology



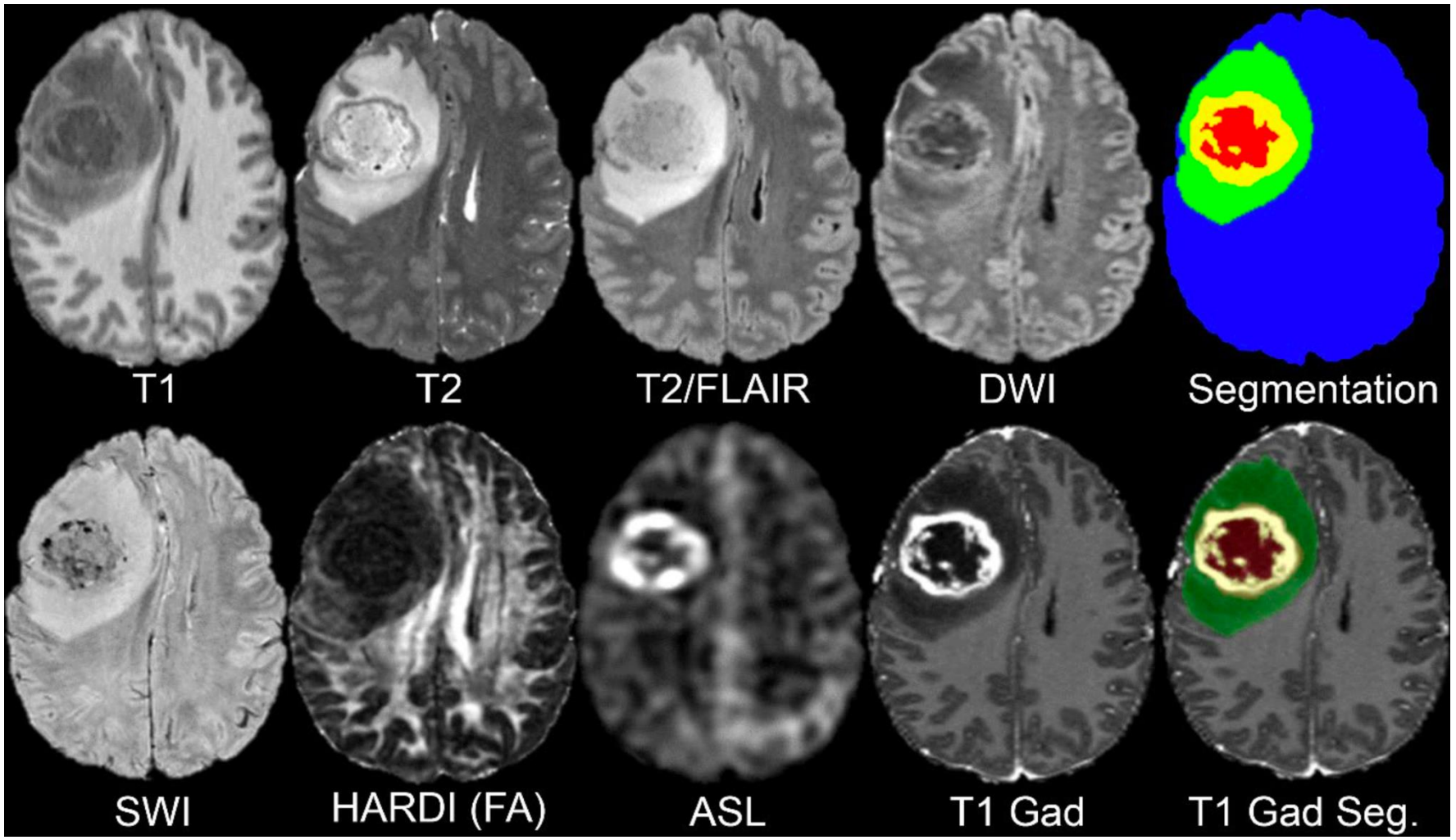
# Glioma in multiparametric MRI (mpMRI)



Tumor sub-regions annotated in the different mpMRI scans

TC: cyan  
ET: yellow  
WT: magenta

The three tumor sub-regions



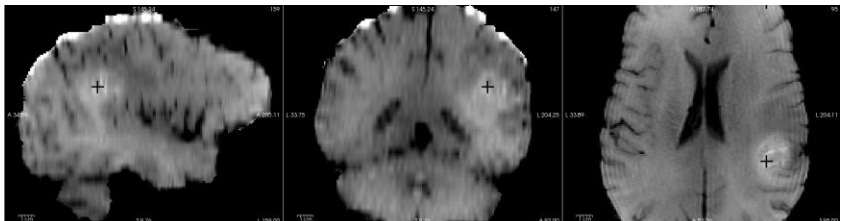
0

1

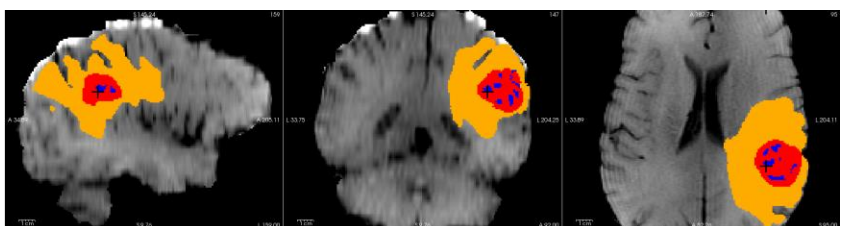
4

2

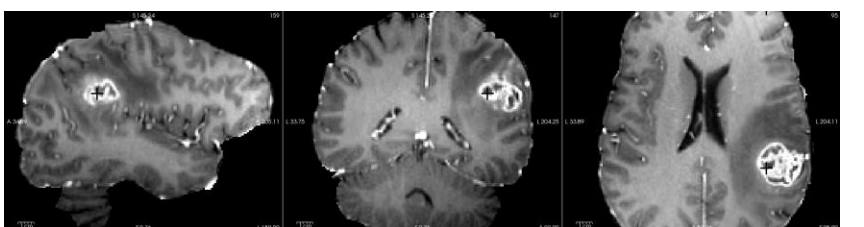
**Bck:** Background; **NCR:** Central non-enhancing and/or necrotic tumor; **ET:** Enhancing tumor (core); **ED:** Surrounding FLAIR abnormality / edema



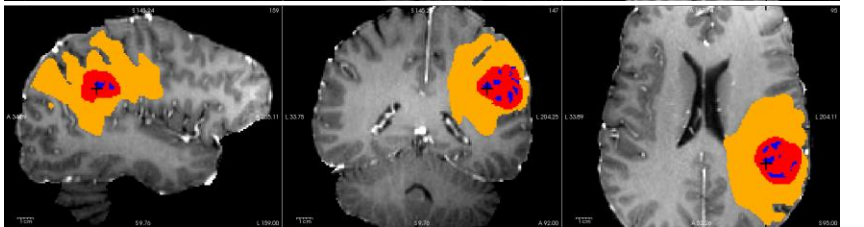
T1



T2

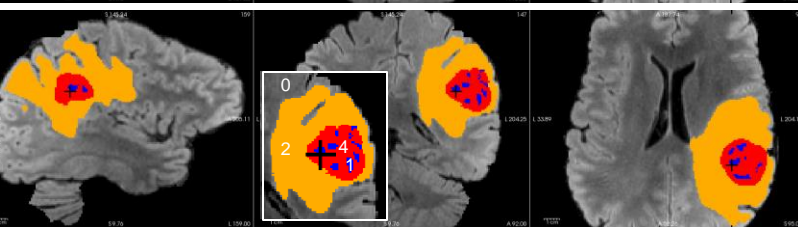
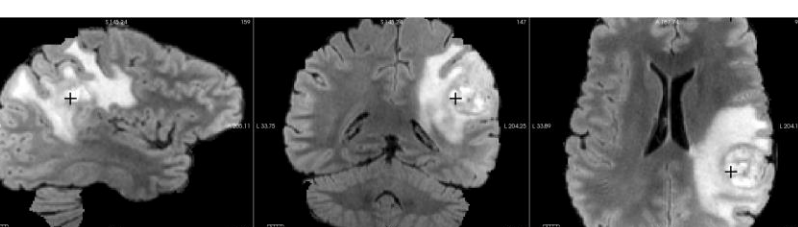
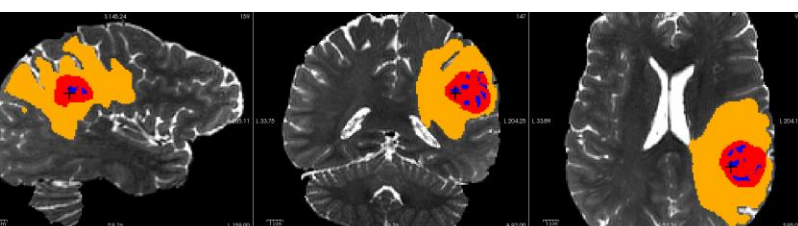
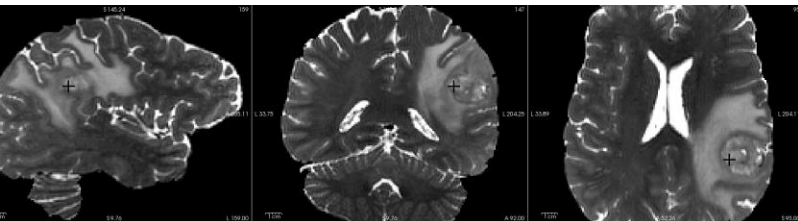


T1c



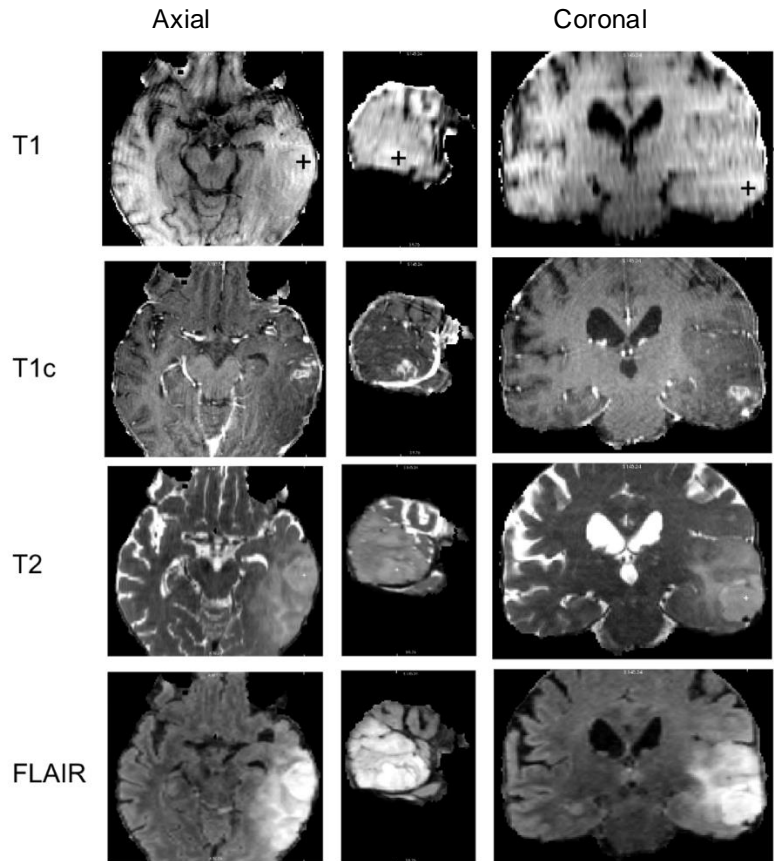
FLAIR

Cursor		-159.37, 92.49, 95.02
RAS		-39.37, 17.52, -26.51
TkReg RAS (UCSF-PDGM-0020_tumor_segmentation.nii)	4	[159, 147, 95]
UCSF-PDGM-0020_tumor_segmentation.nii	733	[159, 147, 95]
UCSF-PDGM-0020_T2.nii	1721	[159, 147, 95]
UCSF-PDGM-0020_FLAIR.nii	972	[159, 147, 95]
UCSF-PDGM-0020_T1.nii	2340	[159, 147, 95]
UCSF-PDGM-0020_T1c.nii		



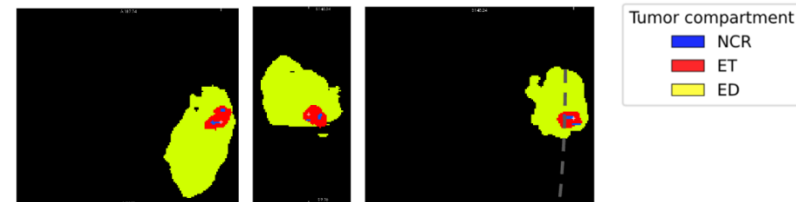
## Acquisition

## The mpMRI recording



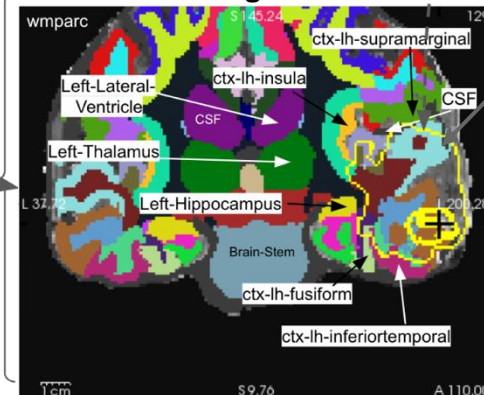
## B rain tumor segmentation

## Three-compartment tumor segmentation mask



## Cortical and subcortical parcellation

wmparc  
semantic segmentation



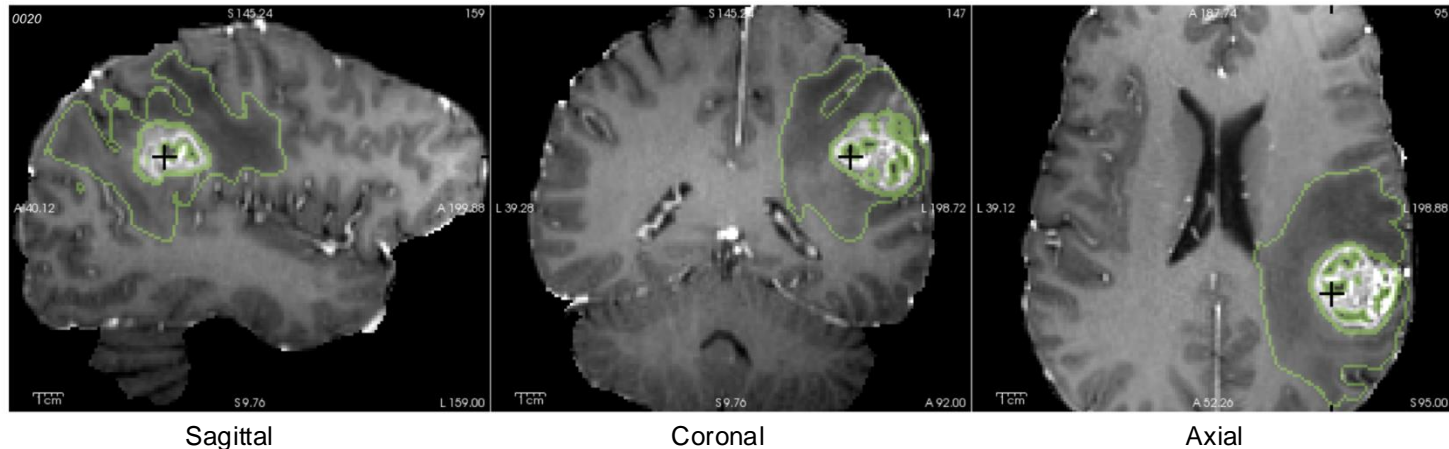
## Boundary of Gross Tumor Volume (GTV)

Normal and abnormal tissue in a coronal plane as annotated color-coded overlays, together with the tumor compartment boundaries

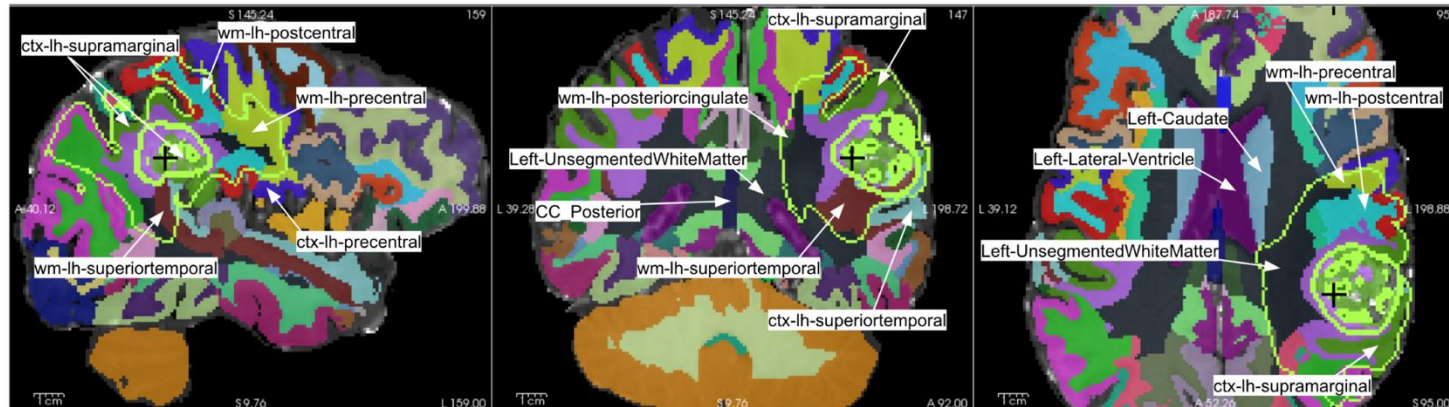
# Tumor location and anatomical neighborhoods obtained by segmentation

( UCSF-PDGM-0020 )

CT1 (Gadolinium contrast)  
with overlay of tumor  
region boundaries



WMPARC (FreeSurfer)  
segmentation with an  
overlay of tumor  
compartment  
boundaries and  
annotation of selected  
anatomical structures  
and regions

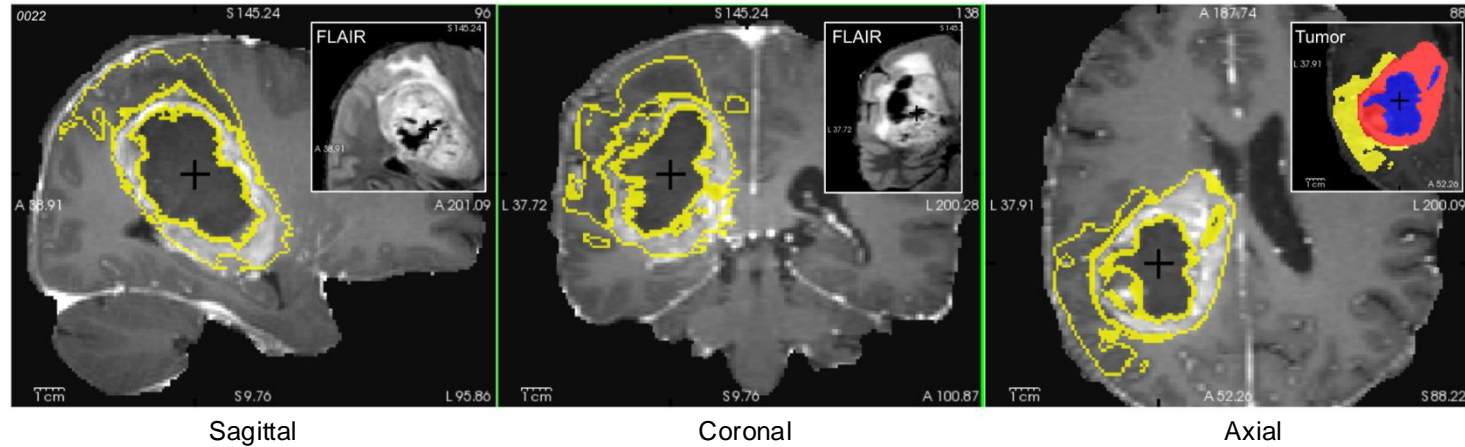


# Tumor location and anatomical neighborhoods obtained by segmentation

( UCSF-PDGM-0022 )

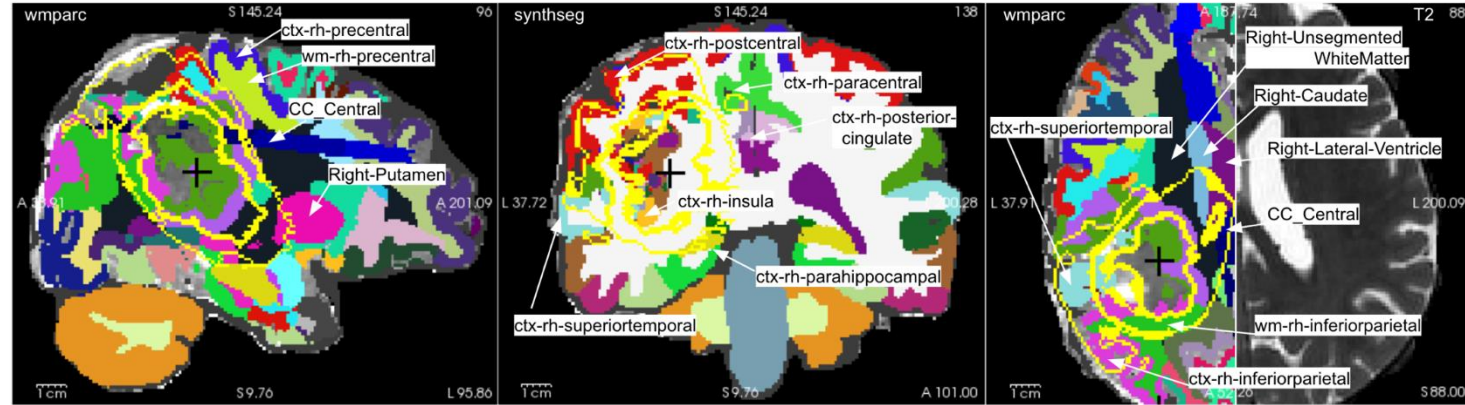
CT1 (Gadolinium contrast)  
with overlay of tumor  
region boundaries.

Inserts:  
The corresponding  
FLAIR (left & middle panels)  
The corresponding 3-  
compartment tumor  
segmentation (right panel)



WMPARC (FreeSurfer)  
segmentation with an  
overlay of tumor  
compartment boundaries  
and annotation of  
selected anatomical  
structures & regions

Right panel:  
The corresponding T2  
in left hemisphere

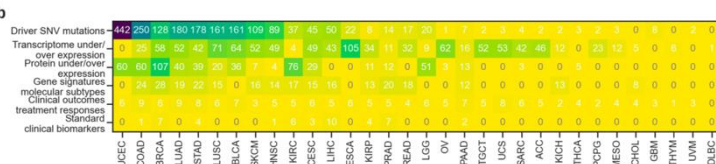
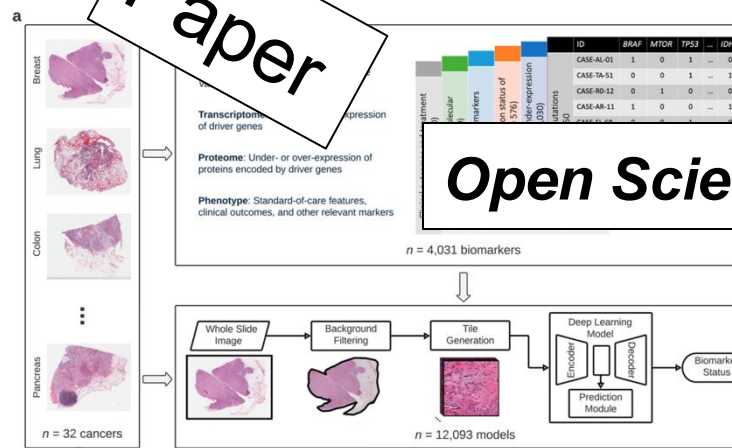


<https://doi.org/10.1038/s43856-024-00471-5>

# A systematic pan-cancer study on deep learning-based prediction of multi-omic biomarkers from routine pathology images

[Check for updates](#)

Salim Arslan <sup>1</sup>, Ju  
Shikha Singh <sup>1</sup>, Ju  
Jakob Nikolas Kal...  
<sup>1</sup> Cher Bass <sup>1</sup>, Debapriya Mehrotra <sup>1</sup>, Andre Geraldes <sup>1</sup>,  
<sup>1</sup> Pandu Raharja-Liu <sup>1</sup>, Oscar Maiques <sup>4,5</sup>,



# A systematic pan-cancer study on deep learning-based prediction of multi-omic biomarkers from routine pathology images

This repo contains the codebase to train and validate an encoder-decoder model for predicting the status of a multi-omic biomarker. It has been used to train and validate the 12,093 models for predicting 4,031 multi-omic biomarkers across 32 cancer types in our multi-omic pan-cancer study. The code allows running end-to-end training and validation for a single biomarker as long as the required

## Pre-requisites

- Ubuntu: 20.04.3 LTS
- Python: 3.6.7

# Open Science & Reproducible Research !

given in the `version_details` file.

## Running the code

### Data preparation and input structure:

- The pipeline is designed to operate on tiles, each is a `numpy.ndarray`. All WSI images used in the study are available at <https://portal.gdc.cancer.gov/>.
- As a pre-requisite, each WSI in the input dataset should be subdivided into patches (tiles).
- Each tile should be of type `numpy.ndarray` and with a shape of `(d x d x 3)`, where `d` is the width and height of a patch and `3` is the number of channels.
- All tiles of an image should be appended into a list, which should then be packed into a python dict, where the key is set to `"img_patches"` as in `{"img_patches": [numpy.ndarray]}`.

# Code

ent with at least  
pip freeze ) are

# Data

slide image (WSI). TCGA images

# scientific data

## OPEN The LUMIERE dataset: Longitudinal Glioblastoma MRI with expert RANO evaluation

Yannick Suter<sup>1,7</sup>✉, Urs peter Knecht<sup>2,7</sup>, Waldo Valenzuela<sup>3</sup>, Michelle Notter<sup>4</sup>, Ekkehard Hewer<sup>5</sup>, Philippe Schucht<sup>6</sup>, Roland Wiest<sup>1,6</sup> & Mauricio Reyes<sup>1,6</sup>✉

<https://www.nature.com/articles/s41597-022-01881-7>

main ▾ 1 Branch 0 Tags Go to file Add file Code

ysuter Update README.md e57c5b4 · last month 9 Commits

Radiomics	Updated collage feat. scripts	last year
Segmentation	Move to public repo	2 years ago
utils	Move to public repo	2 years ago
.gitignore	Initial commit	3 years ago
README.md	Update README.md	last month

README

This repository contains the code used to prepare the data in:

## The LUMIERE Dataset: Longitudinal Glioblastoma MRI with Expert RANO Evaluation

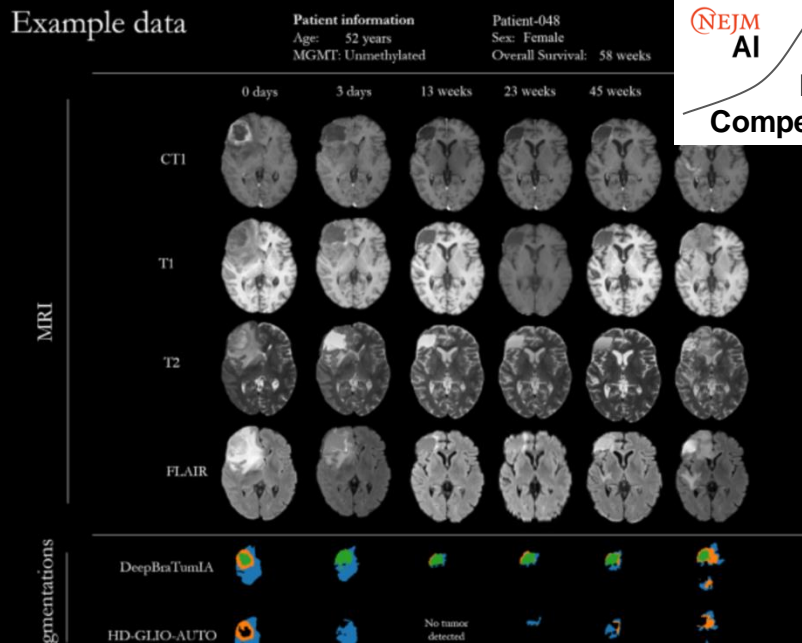
Please cite the following publication when using this dataset:

Suter, Y., Knecht, U., Valenzuela, W., Notter, M., Hewer, E., Schucht, P., Wiest, R. and Reyes, M., 2022. The LUMIERE dataset: Longitudinal Glioblastoma MRI with expert RANO evaluation. *Scientific data*, 9(1), p.768. <https://doi.org/10.1038/s41597-022-01881-7>

The dataset can be downloaded from [Figshare](#). Please note that the data is available for non-commercial use.

<https://github.com/ysuter/gbm-data-longitudinal>

## Example data



figshare.com/s/f3f5429e9e9275ad279d This website uses cookies to help you have a better on-line experience. By using this website, you are agreeing to the use of cookies as explained in our cookie policy. Accept cookies

figshare Browse Search on figshare... Log in Sign up

⋮ The LUMIERE Dataset: Longitudinal Glioblastoma MRI with Expert RANO Evaluation

✓ This collection is shared privately

This is a single-center longitudinal glioblastoma MRI dataset with expert ratings of selected follow-up studies according to response assessment in neuro-oncology criteria (RANO). The expert rating includes details about the rationale of the ratings. For a subset of patients, we provide pathology information regarding methylation of the O6-methylguanine-DNA methyltransferase (MGMT) and isocitrate dehydrogenase 1 (IDH1), as well as the overall survival time. The MRI data includes T1-weighted, T2-weighted, and fluid-attenuated inversion recovery (FLAIR) MRI. Segmentations from state-of-the-art automated segmentation tools (DeepBraTumIA, HD-GLIO-AUTO), as well as radiomic features, complement the imaging data. This collection includes MRI data of 91 GBM patients with a total of 638 study dates and 2487 images. Possible applications of this dataset are radiomics research, the development and validation of automated segmentation methods, and studies on response assessment.

COLLECTION SIZE 80.85 GB

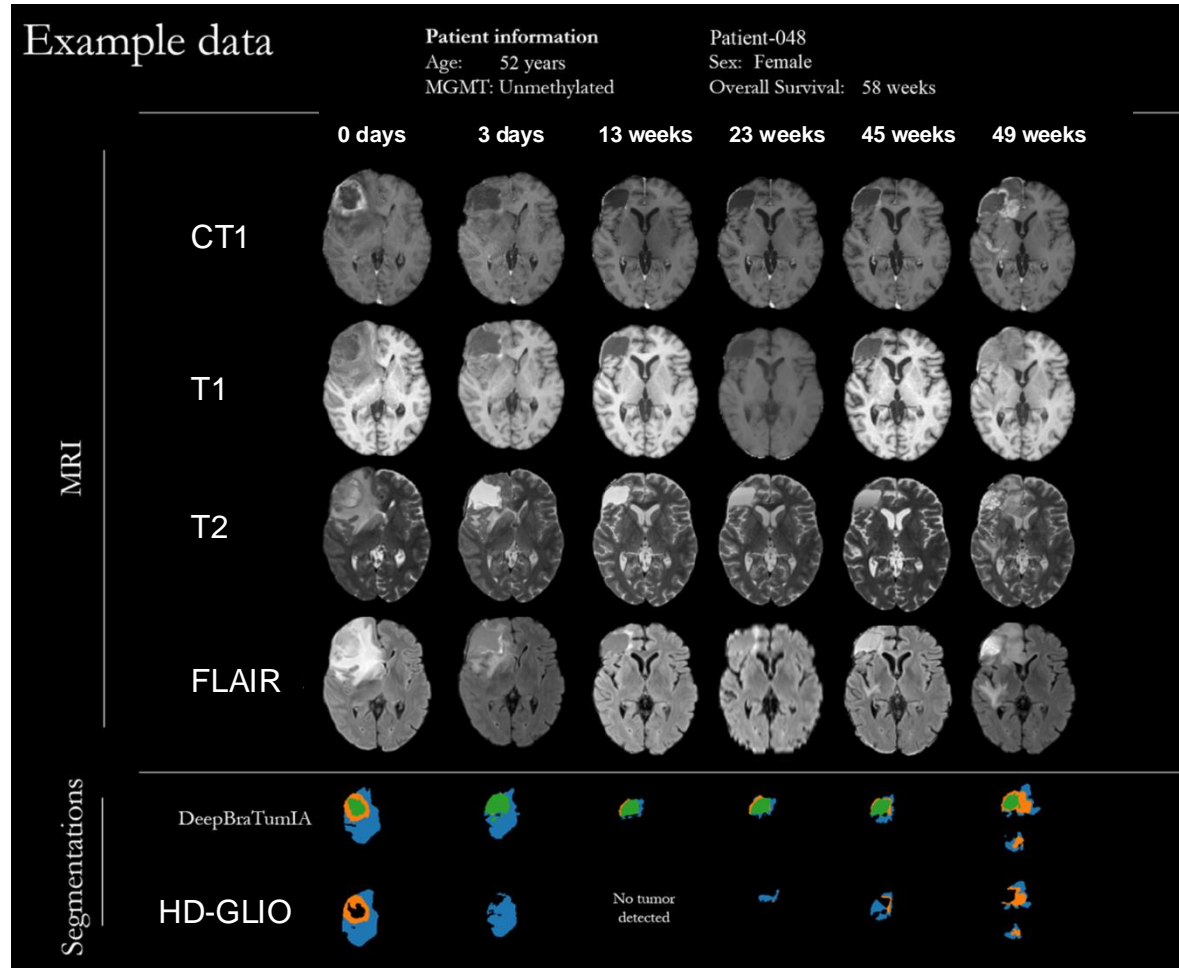
CATEGORIES • Artificial Intelligence and Image Processing • Radiology and Organ Imaging

KEYWORDS Glioblastoma MRI Radiomics Longitudinal data Expert ratings Response assessment Automated segmentation

<https://figshare.com/s/f3f5429e9e9275ad279d>

NEJM  
AI  
Data  
Code  
Papers  
Competitions

# Example data



LUMIERE

Patient-048

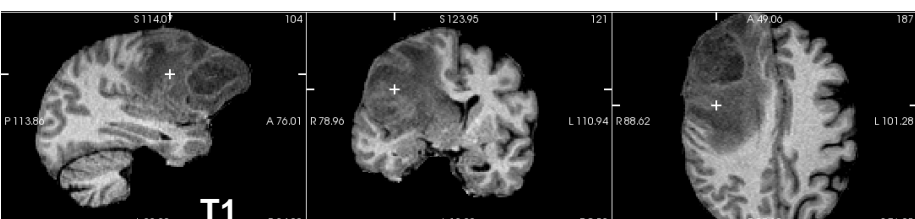
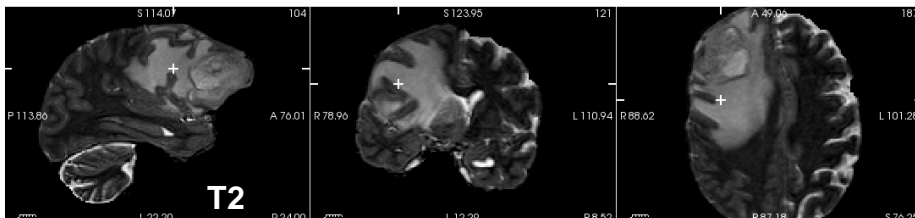
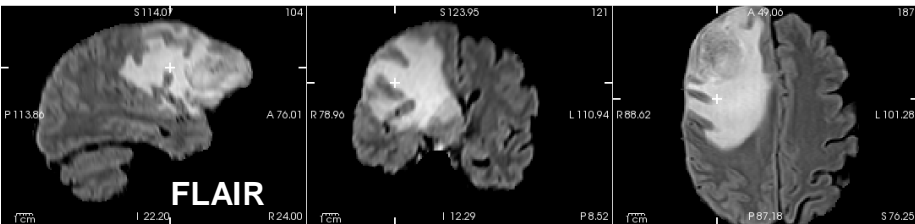
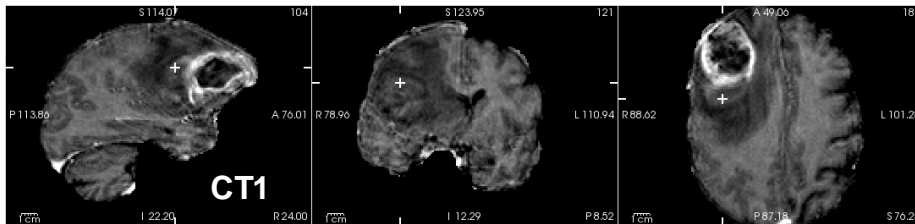
Age: 52 years

Sex: Female

MGMT: Unmethylated

Overall Survival: 58 weeks

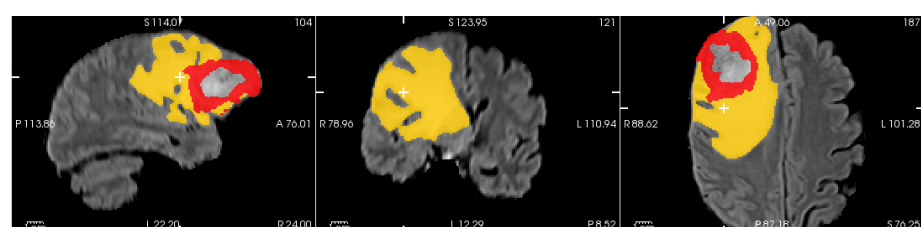
# Multiparametric MRI



Segmentation

HD-GLIO

**CE** ( $\approx$  CT1)  $\cup$  **NE** ( $\approx$  FLAIR)

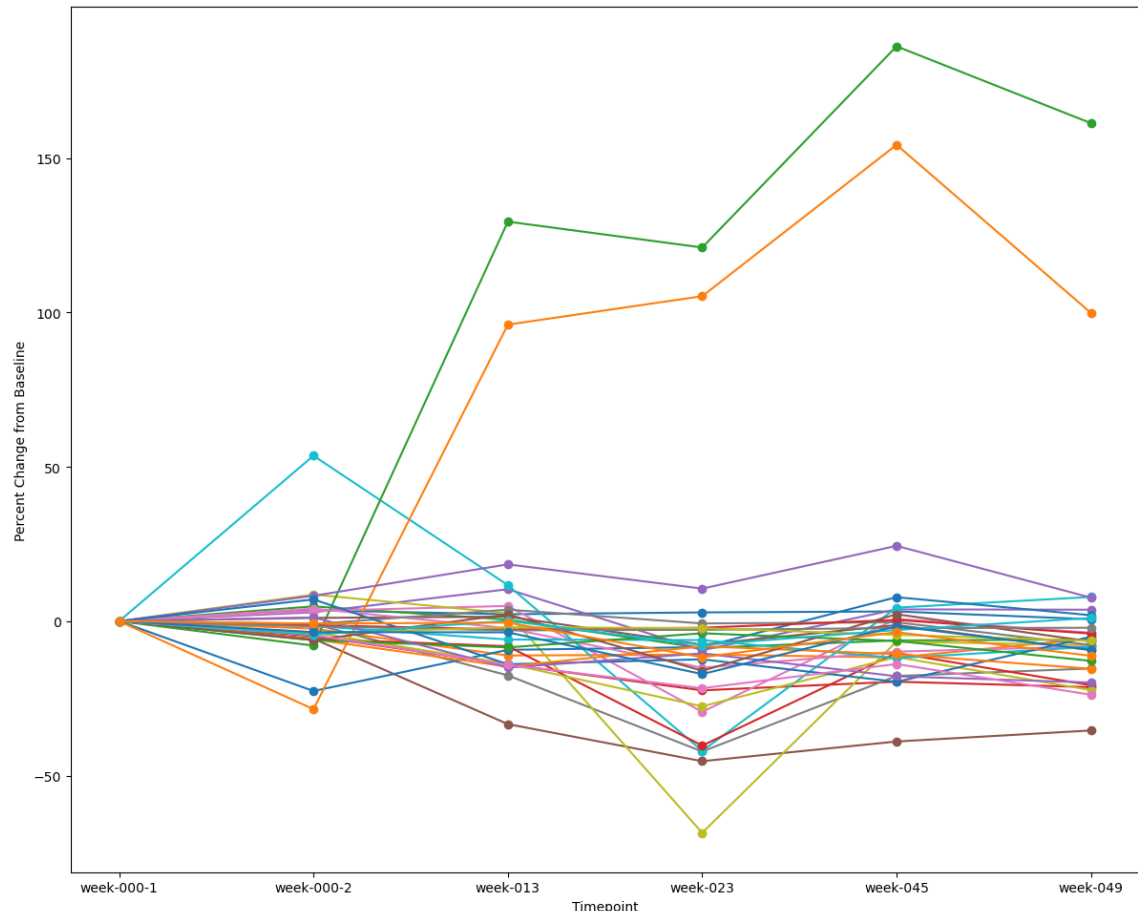


SynthSeg

[Billot et al. Med Im Anal 2023;86:102789](https://doi.org/10.1007/s10278-023-01027-9)



# Regional volume changes over time



- Cerebral\_WM\_Left
- Cerebral\_WM\_Right
- Thalamus\_Left
- Thalamus\_Right
- Caudate\_Left
- Caudate\_Right
- Putamen\_Left
- Putamen\_Right
- Pallidum\_Left
- Pallidum\_Right
- Lateral\_Ventricle\_Left
- Lateral\_Ventricle\_Right
- Third\_Ventricle
- Fourth\_Ventricle
- CSF
- Hippocampus\_Left
- Hippocampus\_Right
- Amygdala\_Left
- Amygdala\_Right
- Frontal\_Left
- Frontal\_Right
- Parietal\_Left
- Parietal\_Right
- Temporal\_Left
- Temporal\_Right
- Occipital\_Left
- Occipital\_Right
- Brainstem
- Cerebellum\_WM\_Left
- Cerebellum\_WM\_Right
- Cerebellum\_Cortex\_Left
- Cerebellum\_Cortex\_Right

cursor (with claude-3.5-sonnet) "Please make an interpretation of the following figure:

`LUMIERE-Patient-048-reg/visualizations/longitudinal\_visualization.png`"

Let me help interpret this figure showing Regional Volume Changes Over Time

for various brain structures:

Key Observations:

### 1. Most Dramatic Changes:

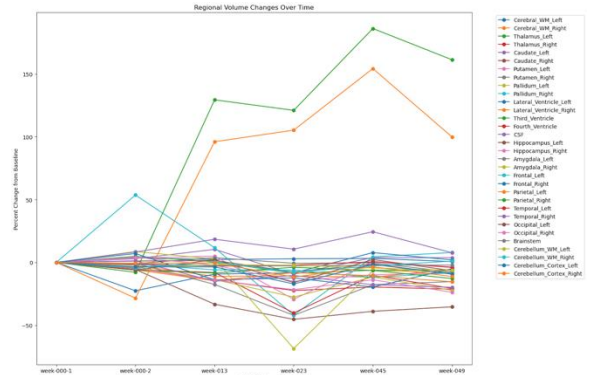
- Lateral\_Ventricle\_Right shows significant expansion (up to ~150% increase by week-045)
- Thalamus\_Left also shows substantial growth (peaks around week-045)
- These changes suggest significant mass effect and potential displacement of structures

### 2. Temporal Pattern:

- Initial stability (week-000-1 to week-000-2)
- Rapid changes between week-000-2 and week-013
- Continued progression through week-045
- Slight regression in some structures by week-049

### 3. Asymmetry:

- Clear left-right asymmetry in several structures
- Particularly notable in ventricles and thalamus
- Suggests unilateral tumor growth/mass effect



### 4. Structure Groups:

- Deep structures (thalamus, ventricles) show largest changes
- Cortical regions show more moderate changes
- Some structures (cerebellum, brainstem) show relative stability

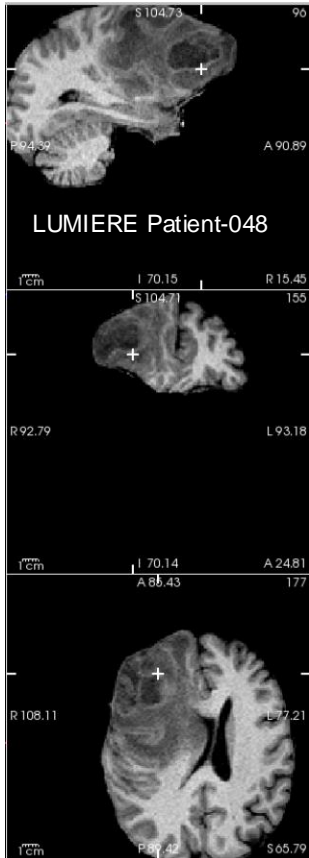
### 5. Clinical Implications:

- Pattern suggests progressive tumor growth with mass effect
- Peak changes around week-045 followed by slight regression might indicate treatment response
- Asymmetric changes could help localize tumor progression

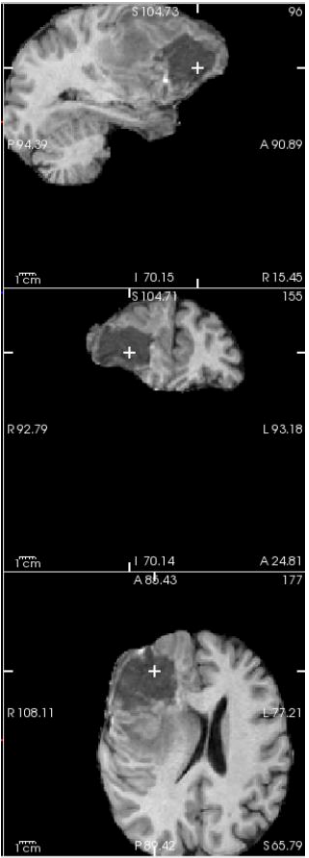
This visualization effectively shows the differential impact of (likely) tumor progression on various brain regions over time, with some structures showing dramatic volume changes while others remain relatively stable.

Would you like me to elaborate on any specific aspect of this interpretation?

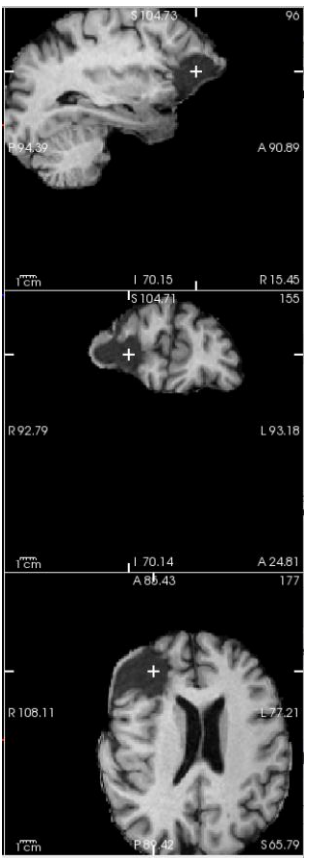
Day 0



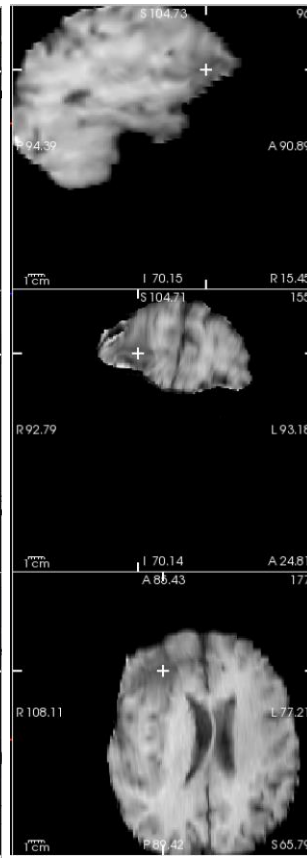
Day 3



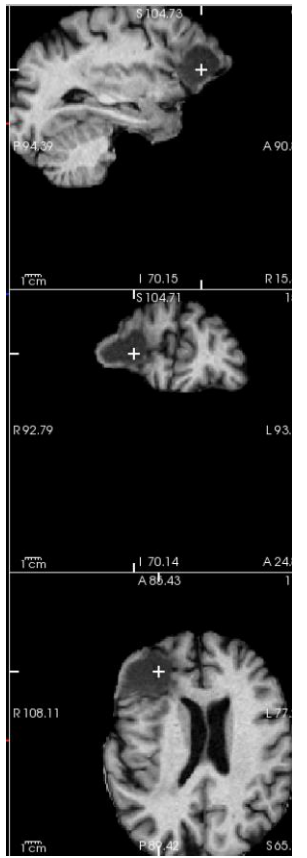
Week 13



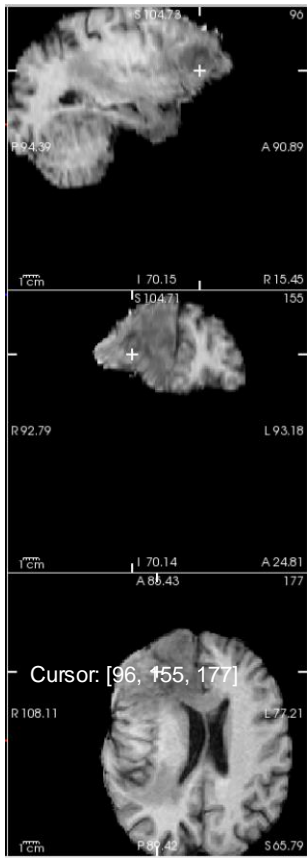
Week 23



Week 45



Week 49





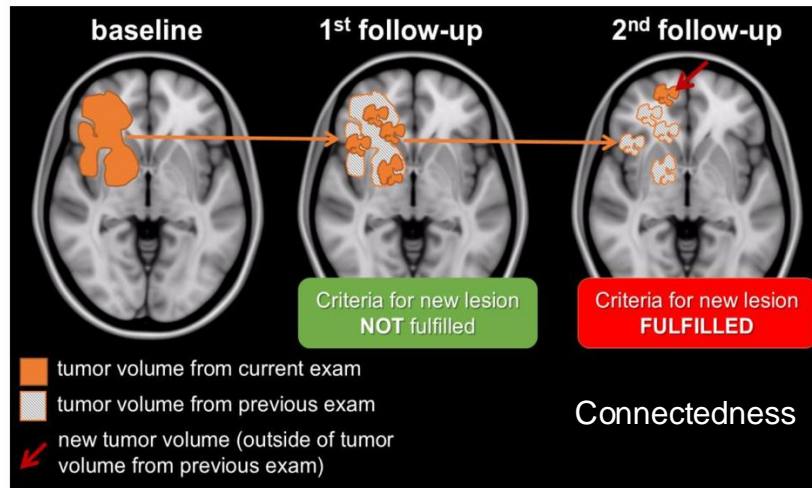
## Automated quantitative tumour response assessment of MRI in neuro-oncology with artificial neural networks: a multicentre, retrospective study

Philipp Kickingereder, MD • Fabian Isensee, MSc • Irada Tursunova, MD • Jens Petersen, MSc •

Ulf Neuberger, MD • David Bonekamp, MD • et al. Show all authors • Show footnotes

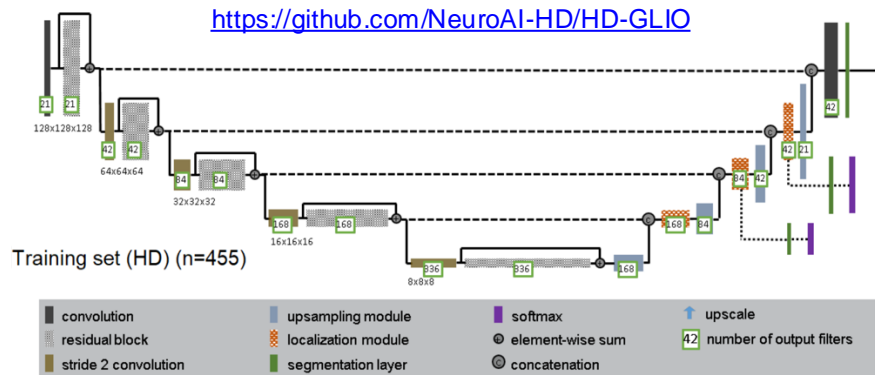
Published: April 02, 2019 • DOI: [https://doi.org/10.1016/S1470-2045\(19\)30098-1](https://doi.org/10.1016/S1470-2045(19)30098-1)

**Supplementary Figure 2.** Schematic illustration of the connected component analysis to enable automated identification of new contrast-enhancing (CE) tumor lesions during follow-up. Analysis is performed outside the boundaries of the CE tumor volume from the preceding MRI exam to disregard those cases where a tumor shrinks into several smaller sub-volumes.



**Supplementary Figure 1.** Artificial neural network (ANN) architecture for automated tumor identification and segmentation on MRI. Our network architecture makes use of the encoder-decoder paradigm first introduced by the U-Net. We use residual connections in the encoder while keeping the decoder as lightweight as possible. Auxiliary segmentation outputs inject gradients deep into the network and facilitate the training of all layers. This network processes 3-dimensional input patches as large as 128x128x128 voxels during training. Its fully convolutional nature is used to predict entire tumor segmentation mask at once at test time, alleviating the need to stitch patches together.

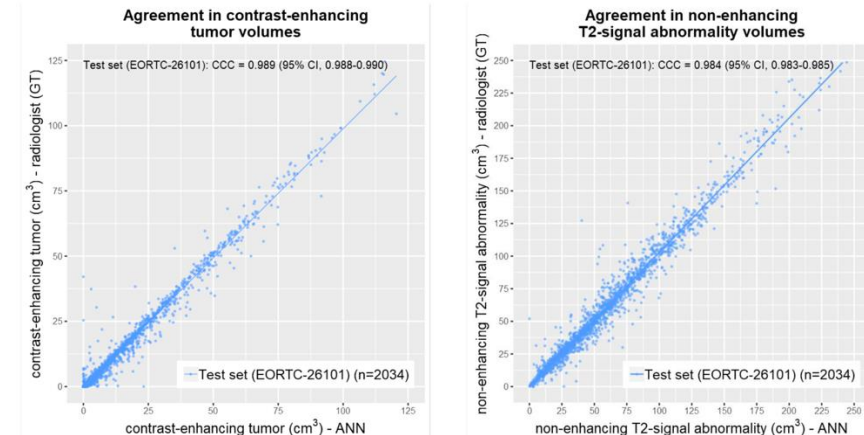
<https://github.com/NeuroAI-HD/HD-GLIO>



Training set (HD) (n=455)

convolution	upsampling module	softmax
residual block	localization module	element-wise sum
stride 2 convolution	segmentation layer	concatenation

▲ upscale  
42 number of output filters



Day 0

**recon-all-clinical**

**FreeSurfer 7.4.1**

**HD-GLIO**

T1

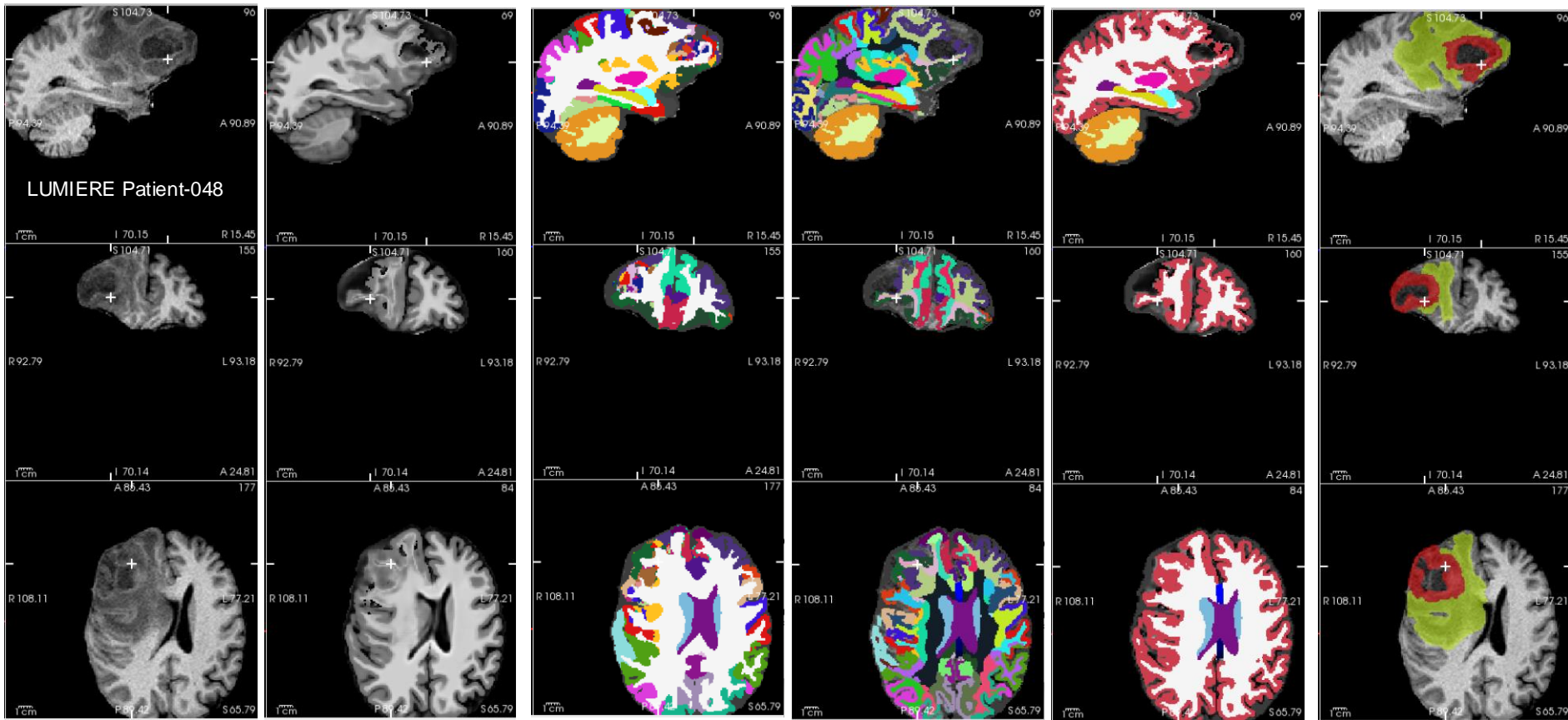
synthSR

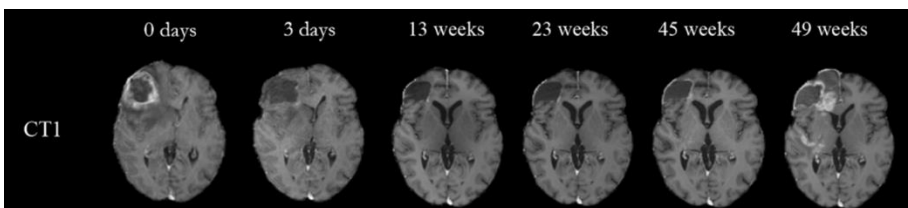
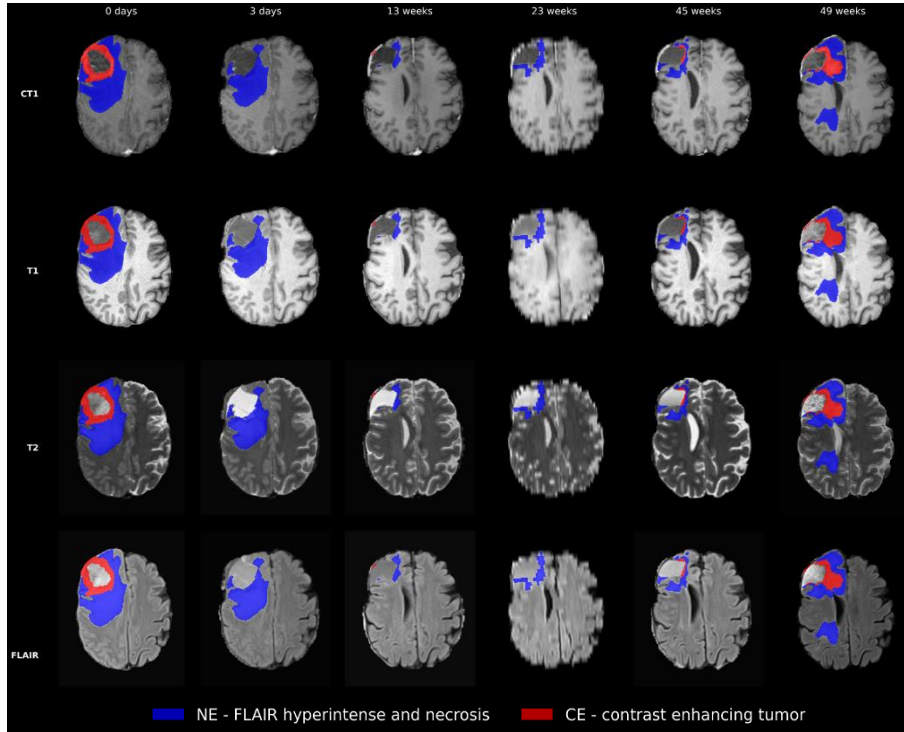
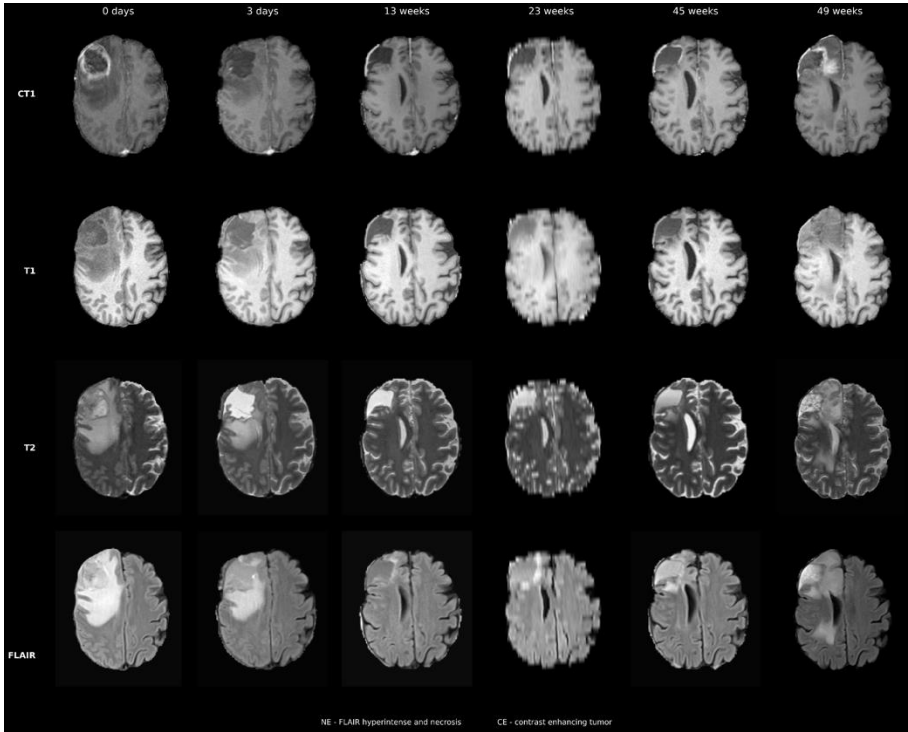
synthseg

wmparc

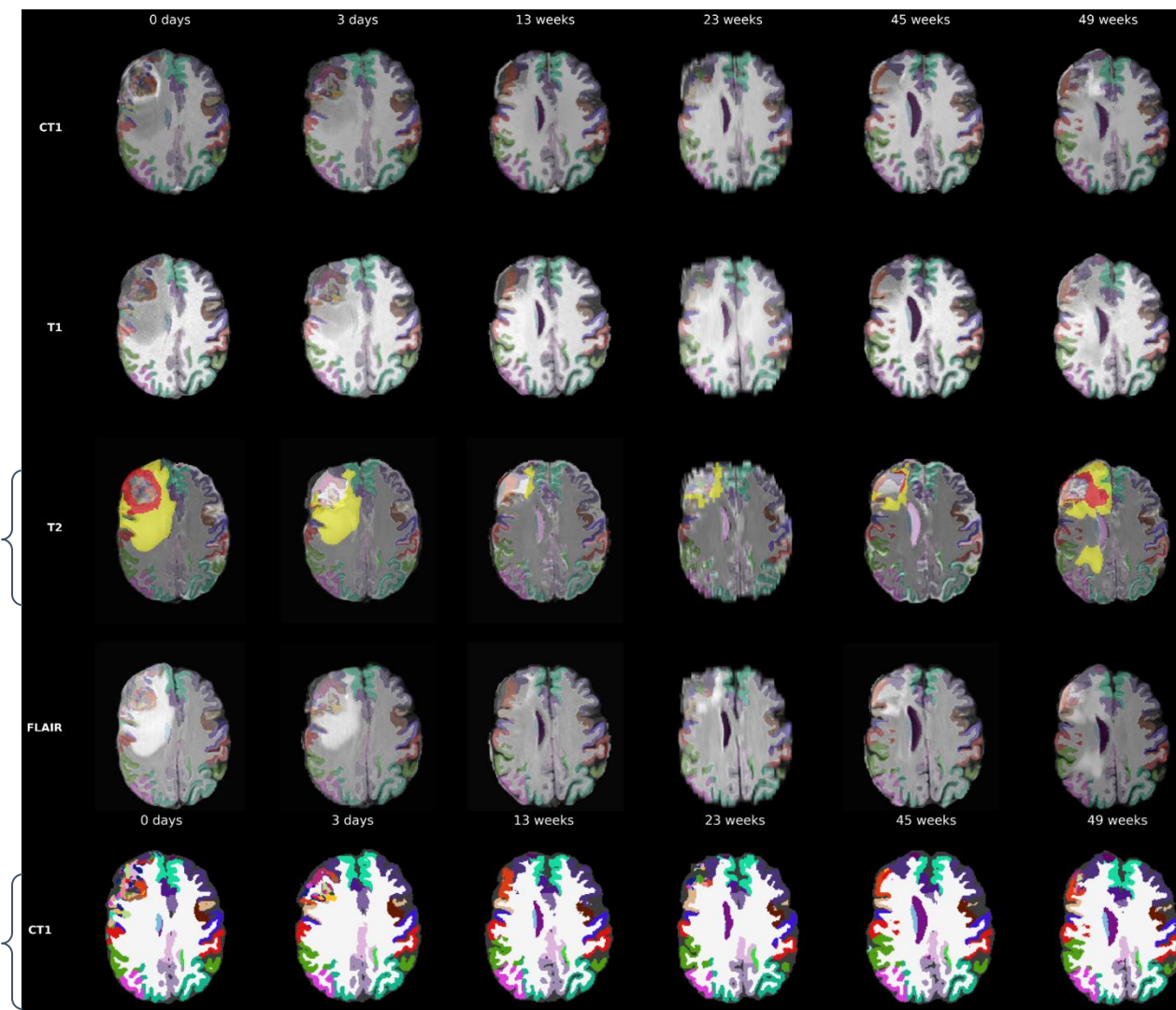
aparc

tumor  
segmentation





<https://github.com/arvidl/glioma-growth>

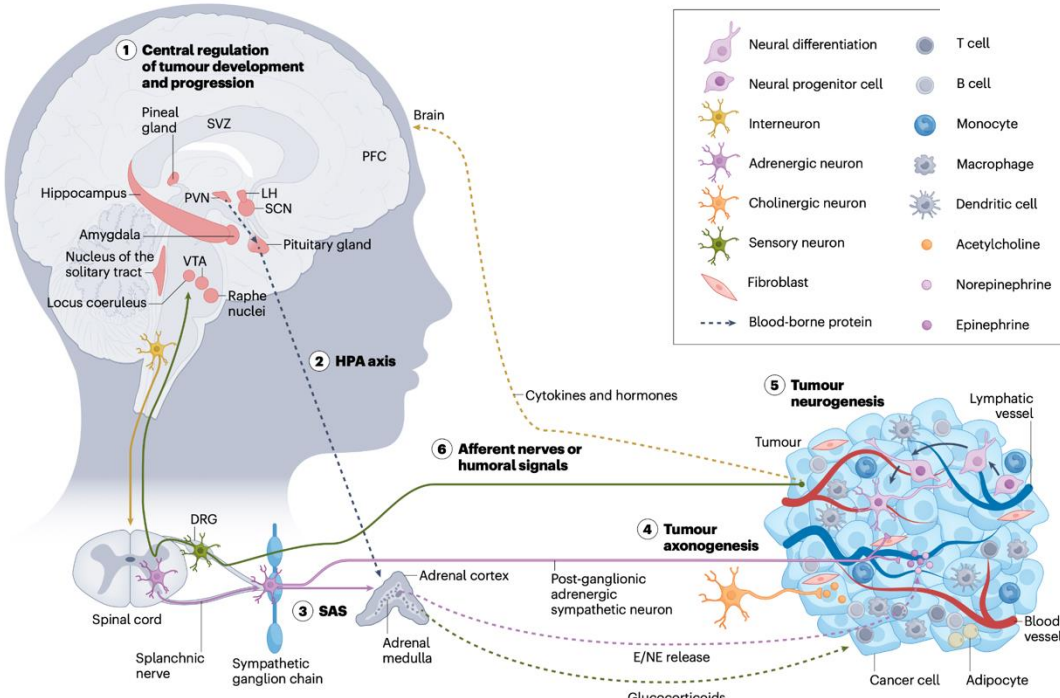


T2 with  
tumor segmentation  
(HD-GLIO) overlay

CT1 with  
Synthseg overlay

# Cancer neuroscience

Magnon & Hondermarck. [The neural addiction of cancer](#). Nat Rev Cancer 2023



Bidirectional crosstalk between the nervous system and solid tumours

nature

nature

Explore content ▾ About the journal ▾ Publish with us ▾

nature > articles > article

Article | [Open access](#) | Published: 03 May 2023

**Glioblastoma remodelling of human neural circuits decreases survival**

Saritha Krishna, Abrar Choudhury, Michael B. Keough, Kyounghee Seo, Liyun Ni, Sofia Kakaizada,

Explore content ▾ About the journal ▾ Publish with us ▾ Subscribe

nature > news & views > article

NEWS AND VIEWS | 03 May 2023

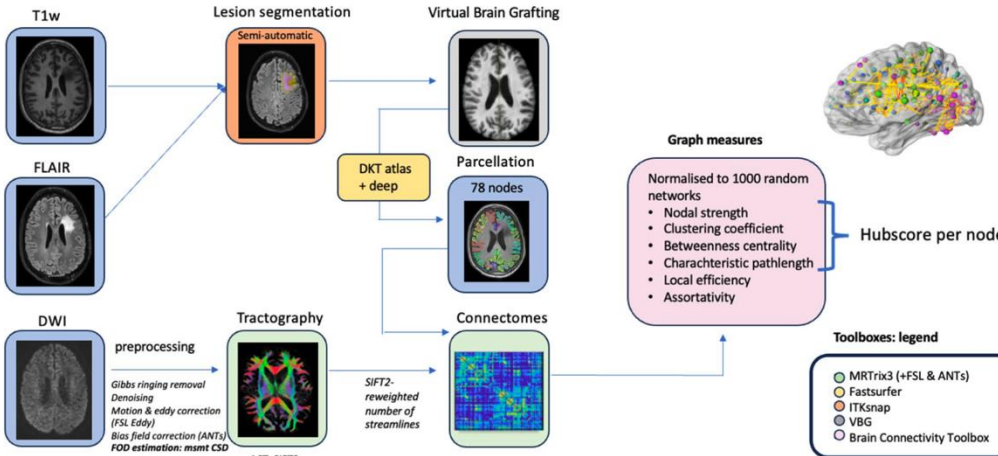
## How thought itself can drive tumour growth

Tumour cells can form connections with neurons in the brain. Examination of a variety of types of evidence concerning human brain cancer sheds light on how these tumour–neuron interactions affect cognition and survival times.

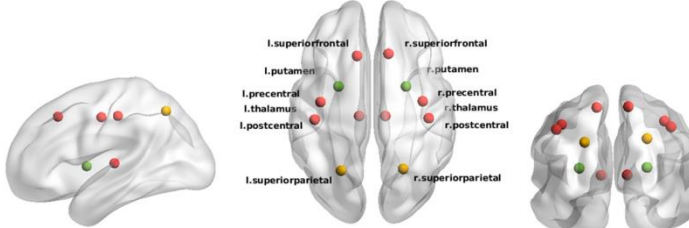
By [George M. Ibrahim](#) & [Michael D. Taylor](#)

Few effective treatments are available for a common and universally fatal type of adult brain tumour called a malignant glioma. Although these tumours exist exclusively in the central nervous system, the interactions between malignant glioma cells and the 86 billion neurons in the human brain are poorly understood. This is particularly relevant because most people with the disease develop progressive cognitive decline that robs them of quality of life during their final months<sup>1</sup>. Writing in *Nature*, Krishna *et al.*<sup>2</sup> show that **malignant gliomas can grow by modifying brain circuitry, thus taking cognitive function away from their host** and ultimately leading to death. These insights might lead to fundamentally new approaches to glioma treatment and provide a means of limiting cognitive decline in affected individuals.

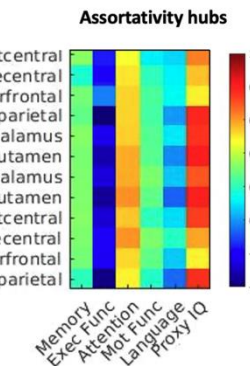
# The role of structural whole-brain and nodal network metrics and their association with cognitive functioning



Imaging processing pipeline. T1 w: T1-weighted images, FLAIR: Fluid-attenuated inversion recovery images, DWI: diffusion-weighted images, FOD: fibre orientation distribution, msmt CSD: multi-shell multi-tissue Constrained Spherical Deconvolution, ACT: anatomically-constrained tractography, DKT: Desikan-Killiany-Tourville atlas.



Hub regions (12 nodes) defined in healthy controls. Nodes defined as hub in both patients and controls are indicated in red. Nodes indicated in yellow (left/right superior parietal) and green (left/right putamen) have a lower likelihood of being a hub in patients than in controls (green: significant difference in frequency between groups, yellow: no significant difference in frequency between groups).



Correlation matrices of cognitive outcomes ( $n=6$ ) per node in hubs for nodal measure of assortativity, i.e. high-degree nodes (hubs) tend to connect to other high-degree nodes.

Cognitive domain	Neurocognitive test
Memory	HVLT-R immediate recall
	HVLT-R delayed recall
	HVLT-R recognition
Executive functioning	TMT B
	SCWT interference
	WAIS IV digit span backwards
Attention / processing speed	WAIS IV sequencing
	WAIS IV symbol substitution
	TMT A
Motor function	SCWT colors
	SCWT words
	WAIS IV digit span forward
Proxy IQ	Grooved pegboard
Language	WAIS IV matrix reasoning
	COWAT semantic
	COWAT phonemic

Cognitive (sub)test grouped per cognitive domain. HVLT-R, Hopkins Verbal Learning Test Revised; TMT, Trail Making Test; SCWT, Stroop Color Word Test; WAIS IV, Wechsler Adult Intelligence Scale, fourth edition; IQ, intelligence quotient; COWAT, Controlled Oral Word Association Test.

# Personalized neuro-oncology

Annu. Rev. Biomed. Eng. 2020. 22:309–41

Annual Review of Biomedical Engineering

## Integrated Biophysical Modeling and Image Analysis: Application to Neuro-Oncology

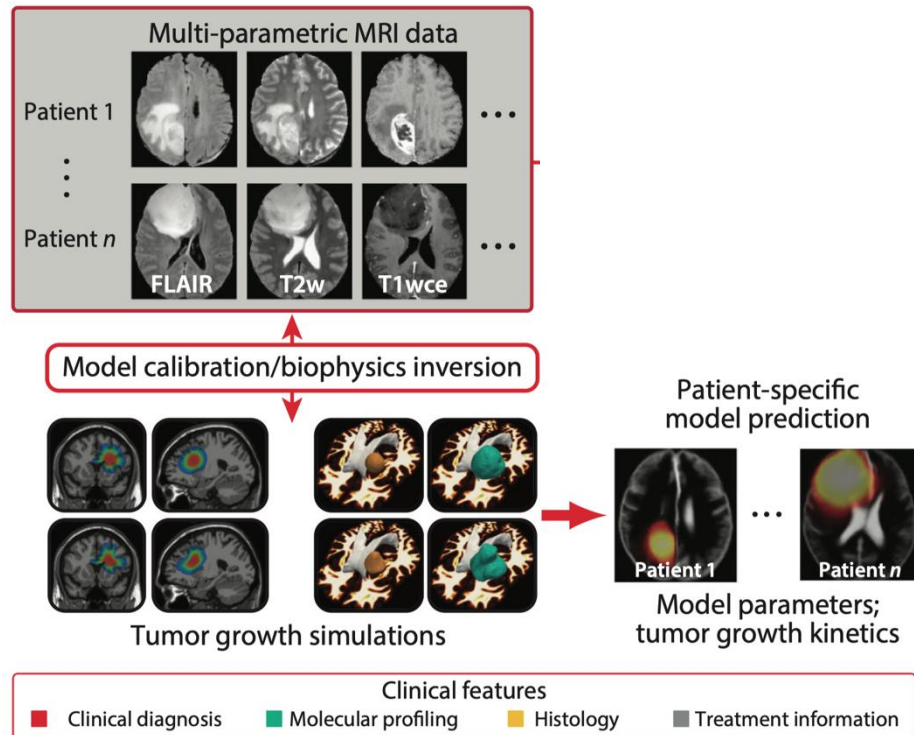
Andreas Mang,<sup>1,\*</sup> Spyridon Bakas,<sup>2,\*</sup>  
Shashank Subramanian,<sup>3</sup> Christos Davatzikos,<sup>2</sup>  
and George Biro<sup>3</sup>

<sup>1</sup>Department of Mathematics, University of Houston, Houston, Texas 77204, USA;  
email: andreas@math.uh.edu

<https://doi.org/10.1146/annurev-bioeng-062117-121105>



# Biophysics modeling of tumor growth (imaging-informed calibration)



- To be clinically useful, biophysical models must be calibrated using the mpMRI information
- Once calibrated, these models can be used to generate patient specific simulations

# Biophysics modeling of tumor growth

A popular hypothesis\* is **go-or-grow**

Tumor progression as (a cycle of) two phases:

- An initially exclusively proliferative phase followed by an invasion of tumor cells into surrounding tissues
- This second phase can then possibly transition back to a proliferating phenotype, which encourages recurrence and growth of metastatic tumors

Kolmogorov, Petrovsky, Piskunov (1937)

The [Fisher-KPP model](#) for tumor growth in the absence of treatment takes the form of a nonlinear **reaction-diffusion type** Partial Differential Equation (PDE) for a **density of tumor cells**  $n = n(\mathbf{x}, t)$  (units number per unit volume):

$$\begin{cases} \frac{\partial n}{\partial t} = \nabla \cdot (\mathbf{D} \nabla n) + \rho n \left(1 - \frac{n}{\kappa}\right) & (\mathbf{x}, t) \in V \times [0, T] \\ n(\mathbf{x}, 0) = n_0(\mathbf{x}) & \text{initial condition at time } t=0 \\ \mathcal{B}n = 0 & \text{zero flux boundary condition} \end{cases}$$

The first term with  $\mathbf{D}$  is a diffusion operator that models the **migration** of cancerous cells into surrounding healthy tissue.

The second term with  $\rho$  models the **proliferation** of tumor cells that can be a logistic growth function

The spatial domain  $V \subset \mathbb{R}^d$  corresponds to the biological domain the tumor is growing in, which we take to be the planar set  $V = [0, 1]^2$  for convenience. The units of  $(\mathbf{x}, t)$  are centimeters and days, respectively, and the units of all other quantities follow by dimensional analysis.

\* H. Hatzikirou et al. 'Go or grow': the key to the emergence of invasion in tumour progression? *Mathematical Medicine and Biology* 2012;29(1):49-65.

\*\* R. Everett et al. A tutorial review of mathematical techniques for quantifying tumor heterogeneity. *Mathematical Biosciences and Engineering* 2020;17(4):3660-3709 <https://www.aimspress.com/article/10.3934/mbe.2020207>

# Simulation using synthetic data

cursor (with claude-3.5-sonnet)

"Explain the code above mathematically (using LaTeX), and the numerical scheme used to solve the PDE."

Here's a mathematical explanation of the code and the numerical scheme:

**1. Fisher-KPP Equation:** The model uses the Fisher-KPP equation for tumor growth:

$$\frac{\partial n}{\partial t} = \nabla \cdot (D(x)\nabla n) + \rho n(1 - \frac{n}{\kappa})$$

“Go-or-Grow”

Where:

- $n(x, t)$ : Tumor cell density
- $D(x)$ : Space-dependent diffusion coefficient
- $\rho$ : Proliferation rate
- $\kappa$ : Carrying capacity

**2. Numerical Scheme:** The PDE is solved using:

- Finite differences for spatial derivatives
- Forward Euler for time integration

The discretization:

$$n_{i,j,l}^{k+1} = n_{i,j,l}^k + \Delta t \left[ D_{i,j,l} \Delta n_{i,j,l}^k + \rho n_{i,j,l}^k \left(1 - \frac{n_{i,j,l}^k}{\kappa}\right) \right]$$

where the discrete Laplacian  $\Delta n_{i,j,l}^k$  is:

$$\Delta n_{i,j,l}^k = \frac{n_{i+1,j,l}^k + n_{i-1,j,l}^k + n_{i,j+1,l}^k + n_{i,j-1,l}^k + n_{i,j,l+1}^k + n_{i,j,l-1}^k - 6n_{i,j,l}^k}{\Delta x^2}$$

## 8. Key Parameters:

- Spatial step:  $\Delta x = \Delta y = \Delta z = 1.0$  mm
- Time step:  $\Delta t = 0.1$  day
- Proliferation rate:  $\rho = 0.2$  day $^{-1}$
- Carrying capacity:  $\kappa = 1.0$
- Diffusion coefficients:
  - White matter:  $D_{wm} = 0.5$  mm $^2$ /day
  - Gray matter:  $D_{gm} = 0.1$  mm $^2$ /day
  - CSF:  $D_{csf} = 0.0$  mm $^2$ /day

By prompting a genAI model

### 3. Tissue-Dependent Diffusion:

```
def tissue_diffusion_map(t1_data):
    # White matter: higher diffusion
    D_wm = 0.5 # mm^2/day
    # Gray matter: lower diffusion
    D_gm = 0.1 # mm^2/day
    # CSF: no diffusion
    D_csf = 0.0 # mm^2/day
```

4. Stability Condition: For numerical stability (CFL condition):  $\Delta t \leq \frac{\Delta x^2}{2D_{max}}$

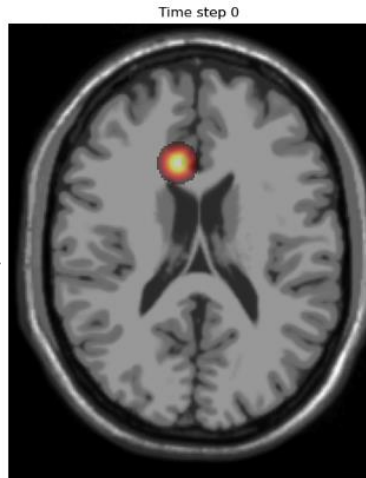
where:

- $d$ : number of dimensions (3 in this case)
- $D_{max}$ : maximum diffusion coefficient

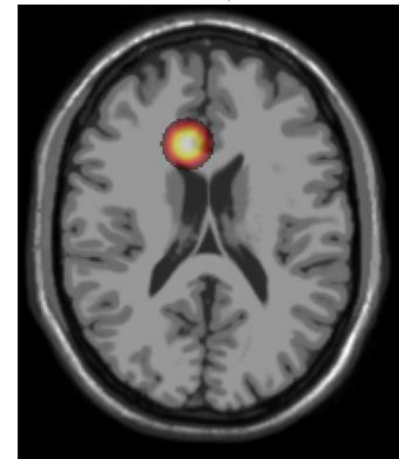
### 5. Implementation in Code:

```
def fisher_kpp_3d(tumor, D_map, rho=0.2, K=1.0, dt=0.1, n_steps=100):
    n = tumor.copy()
    dx = dy = dz = 1.0

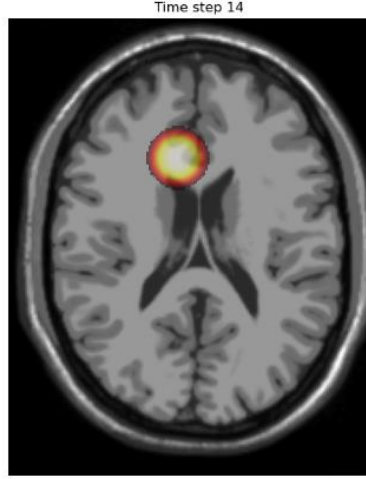
    # Time evolution
    for t in range(n_steps):
        # Compute Laplacian with tissue-dependent diffusion
```



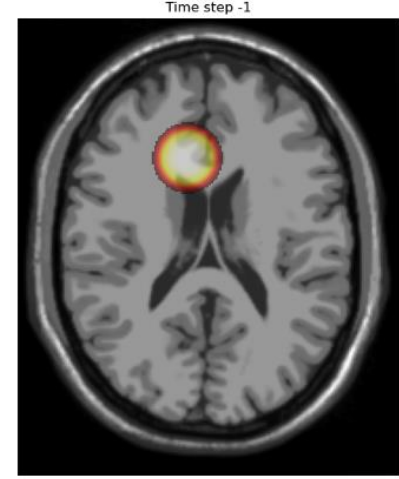
Time step 0



Time step 7



Time step 14

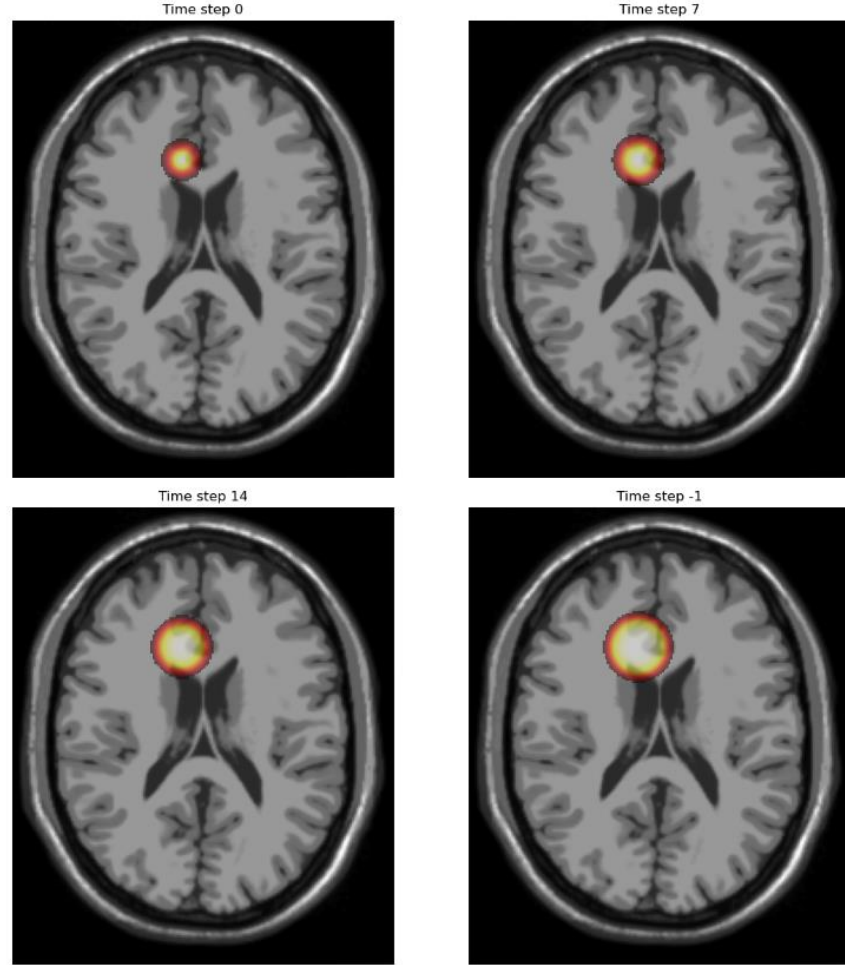
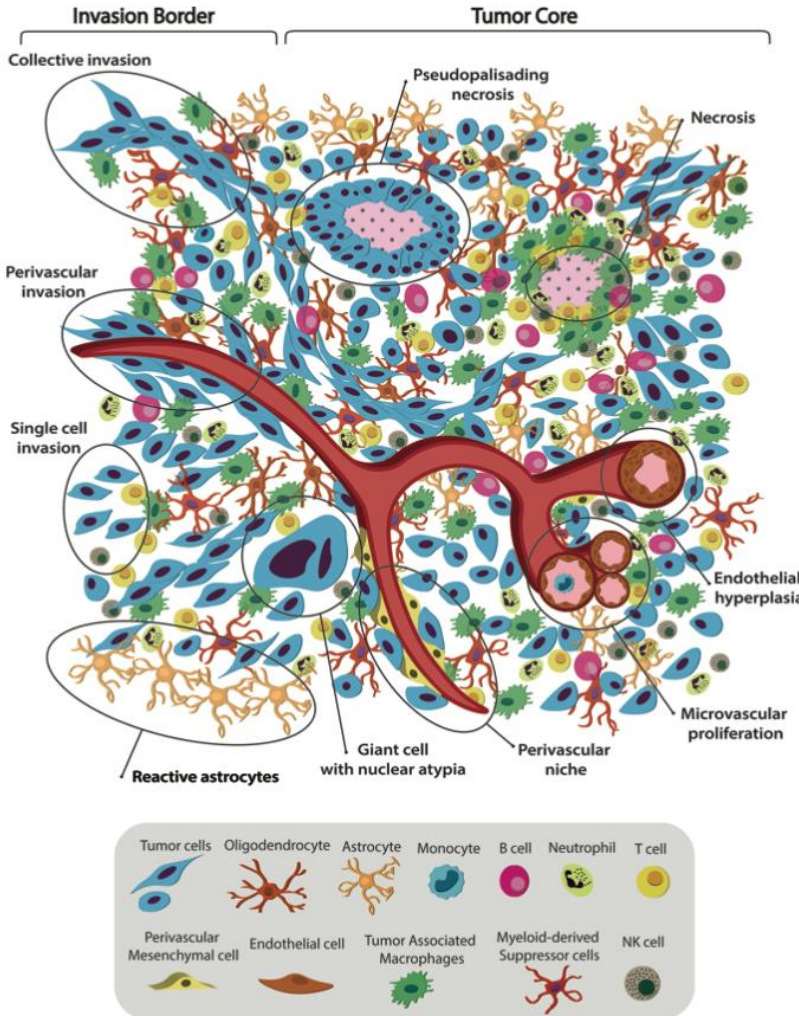


Time step -1

CPU times: user 1min 8s, sys: 14.7 s, total: 1min 23s  
Wall time: 1min 24s

BrainWeb download: T1 ICBM normal 1mm pn0 rf0

<https://github.com/arvidl/glioma-growth>



CPU times: user 1min 8s, sys: 14.7 s, total: 1min 23s  
Wall time: 1min 24s

BrainWeb download: T1 ICBM normal 1mm pn0 rf0

A scenic view of a Norwegian fjord town. In the foreground, a large body of water features a fountain with multiple jets of water. To the right, there's a modern building complex with a white cylindrical tower and a green sphere on top. The word "CODE" is visible on one of the buildings. In the background, there are several hills covered in green vegetation and numerous houses built on the slopes. The sky is clear and blue.

Thank you !